Supplement of Atmos. Chem. Phys., 25, 3049–3107, 2025
https://doi.org/10.5194/acp-25-3049-2025-supplement

Atmospheric Chemistry and Physics
Open Access

Supplement of

Critical load exceedances for North America and Europe using an ensemble of models and an investigation of causes of environmental impact estimate variability: an AQMEII4 study

Paul A. Makar et al.

Correspondence to: Paul A. Makar (paul.makar@ec.gc.ca)

Contents:

S1.0 Background information – Introduction to the Critical Load concept, and detailed descriptions of the CL data used in this work

As noted in the main document, a critical load in this context was defined (Nilsson and Grennfelt, 1988) as "A quantitative estimate of an exposure to one or more pollutants below which significant harmful effects on specified sensitive elements of the environment do not occur, according to present knowledge".

The Nilsson and Grennfelt (1988) definition is worthy of parsing in order to ensure understanding of its implications in context to the present work, and doing so will aid in the interpretation of our analysis results.

With regards to "exposure to one or more pollutants", both sulphur and nitrogen-containing compounds are considered to be relevant for acidification, and these may be deposited in different forms. Sulphur is deposited as gaseous sulphur dioxide (SO_2 dry deposition), as sulphate or bisulphite ions in precipitation (SO_4^{2-} and HSO_3^- wet deposition), or when particles containing sulphate reach and remain on the surface (particulate sulphate dry deposition). Nitrogen deposition comprises a larger number of chemical species, with contributions of dry deposition of gases (nitrogen dioxide (NO_2), nitric acid (HNO_3), ammonia (NH_3), peroxyacetylnitrate (PAN), organic nitrates (a host of possible species), dinitrogen pentoxide (N_2O_5), pernitric acid (HNO_4) and nitrogen monoxide (NO), and a variety of other species in low concentrations), nitrate and ammonium ions in precipitation (NO_3^- and NH_4^+ wet deposition), and dry deposition of particulate nitrate and ammonium. Chemical transport models (CTMs) must therefore accurately estimate the sulphur and nitrogen containing species' emissions, transport, chemical reactions (gaseous, particulate, aqueous), cloud processing (uptake of gases and aerosols into hydrometeors such as cloud water, rain, snow, graupel, etc), precipitation (transfer of the resulting chemically transformed species to the surface of the earth during precipitation events), and removal fluxes at the surface (dry deposition). The manner in which these complex processes are carried out depends on the implementation details of the specific CTM. As atmospheric science progresses, the process representation of the CTMs changes and improves. Estimates of environmental impacts of deposition may thus also change over time, not just in response to changes in emissions and other atmospheric and environmental conditions, but also due to the gradual progress of air-quality modelling science.

With regards to "according to present knowledge" – this part of the definition also acknowledges that knowledge changes over time. The underlying data used in estimating critical loads may improve – for example by including chemical species previously believed to have an insignificant impact on exceedances (Liggio *et al.*, 2024). The CTMs used to generate deposition fluxes for critical load development and critical load exceedance (CLE) estimates are frequently updated, with new process representation, which in turn may lead to changes in the predicted deposition fluxes. The emissions inputs to the models may also change, reflecting better emissions data collection, the enactment of emissions control legislation, changing environmental conditions (year to year variability in meteorology, as well as climate change), and changes in the quality of land use and proxy data used to determine both emissions and deposition fluxes. These changes imply the need to carry out critical load exceedance calculations on an ongoing basis, so that the estimation of ecosystem impact assessments makes use of the most recent science and best available input data.

With regards to "below which *significant* harmful effects on specified sensitive elements of the environment do *not* occur,": the usual approach in defining critical loads is to set, in advance, a level of ecosystem change that is expected to have negative effects on connected components or ecosystem services. Typically, the pollutant loading corresponding to a certain level of ecosystem damage is used (e.g., the amount of acidifying deposition at which 90 or 95% of sensitive species remain undamaged despite the given deposition level, the amount of N deposition resulting in 80% of sensitive plant species remaining undamaged, etc.; CLRTAP, 2023). Critical load values vary across the landscape and ecosystem components. For example, lichen communities are very sensitive to small changes, while herbaceous communities have natural buffers that require higher levels of deposition before species are lost (Simkin *et al.,* 2016, Geiser *et al.,* 2019). Potential ecosystem damage is considered to be "significant" above this level of deposition – but deposition below the critical load does not imply an *absence* of potential ecosystem damage.

1.1 North American Forest Soil Critical Loads of Acidity using the Steady-State Mass Balance Model

Forest soil critical loads maps were assembled from several studies within the U.S. and Canada (Figure S1 and Table S1). Critical loads were (in all but one study) calculated using the Steady-State (or Simple) Mass Balance (SMB) model (Sverdrup & Warfvinge, 1990; Sverdrup & De Vries, 1994) which has simple input parameter requirements and assumes the ecosystem is at long-term equilibrium. The SMB model defines the critical load as a line connecting three points in (S_{dep}, N_{dep}) space, $CL_{max}S$ (the maximum sulphur critical load), $CL_{max}N$ (the maximum nitrogen critical load) and the $CL_{min}N$ (the minimum nitrogen critical load). The regions above the (S_{dep}, N_{dep}) line connecting the points ($CL_{max}S,0$), ($CL_{max}S,CL_{min}N$) and ($0,CL_{max}N$) are said to be in exceedance of the critical load (see Figure 1). $CL_{max}S$ is determined by alkaline inputs to the ecosystem such as base cation deposition (BC_{dep}) and base cation weathering (BC_w) minus acidic inputs (chloride deposition, Cl_{dep}), losses through (non-sodium) base cation uptake through harvesting or grazing (BC_u) (Equation 1), and the critical leaching of the acid neutralizing capacity ($ANC_{le,crit}$, Equation 2).

$$CL_{max}S = BC_{dep} + BC_w - Cl_{dep} - BC_u - ANC_{le,crit} \quad (1)$$

$$ANC_{le,crit} = -Q^{2/3} \cdot \left(1.5 \cdot \frac{Bc_{dep} + Bc_w - Bc_u}{K_{gibb} \cdot (Bc/Al)_{crit}}\right) \quad (2)$$

The Acid Neutralizing Capacity refers to the soil's ability to neutralize input fluxes of acidifying ions through the release of cations from the soil into the soil water. The addition of these neutralizing ions to soil water is a process known as leaching. However, the removal of base cations from soil water may also result in damage to plants via reductions in root growth, stem growth and crops, with the extent of damage dependent on the plant species. The plant-species-specific critical base cation to aluminum soil water ratio in equation (2), $(Bc/Al)_{crit}$, is linked to corresponding precent reductions of plant growth. If a larger percent reduction is deemed acceptable, the value of $(B_c/Al)_{crit}$ will be smaller, the magnitude of $ANC_{le,crit}$ will be larger, and the value of $CL_{max}S$ will be larger, and larger amounts of deposition will be required to exceed the critical load. Conversely, if a smaller impact is deemed acceptable, the value of $(B_c/Al)_{crit}$ will be larger, the magnitude of $ANC_{le,crit}$ will be smaller, the value of $CL_{max}S$ will be smaller, and smaller amounts of deposition will be required to exceed the critical load. Examples of $(Bc/Al)_{crit}$ values for different tree types and ground vegetation may be found in CLRTAP (2023), Chapter V, Table V.8). The critical base cation to aluminum ratio, $(B_c/Al)_{crit}$ (multiplied by the gibbsite equilibrium constant K_{gibb}) is thus the chemical criterion usually used to define the acceptable level of potential damage to biota, specifically via the definition of $ANC_{le,crit,}$ which includes the effect of soil runoff (Q).

The $CL_{min}N$ represents the long-term removal of N from the ecosystem as defined by nitrogen immobilization (N_i) and uptake (N_u) (Equation 3). The $CL_{max}N$ value is determined using $CL_{min}N$ and $CL_{max}S$, which is divided by unity minus the denitrification fraction (f_{de}) (Equation 4). Deposition points of S_{dep} and N_{dep} which fall outside (above) the critical load exceedance line defined by $Cl_{min}N$, $CL_{max}N$, and $CL_{max}S$ are considered to be in *exceedance of their critical loads* (see Figure 1, Regions 1 through 4). Note that these critical loads may be specific to a political jurisdiction, and hence caution should be applied when considering the critical loads and exceedance maps where there are cross-border discontinuities in data sources, parameterization and methodology, and resolution.

$$CL_{min}N = N_i + N_u \quad (3)$$

$$CL_{max}N = CL_{min}N + \left(\frac{CL_{max}S}{(1-f_{de})}\right) \quad (4)$$

Figure S1 illustrates the manner in which critical loads with respect to acidity are calculated using the SMB methodology. Based on the sulphur and nitrogen deposition amounts (S_{dep}, N_{dep}), the Region in which exceedance is occurring is first defined. The amount of exceedance is defined as the shortest possible path (in eq of deposition) to the shaded "no-exceedance" Region 0 of Figure S1, bordered by the line described above. Deposition amounts which fall above the critical load function defined by Region 0 are considered to be in exceedance of their critical loads. The shape of the critical load function is defined by $CL_{max}S$, $CL_{min}N$ and $CL_{max}N$, which in turn are functions of the ecosystems and at-risk species under consideration.

Four Regions are displayed in the Figure. Region S1 corresponds to locations where nitrogen deposition has exceeded the $CL_{max}N$ value and sulphur deposition is always greater than $CL_{max}S$: the only means by which exceedances can be reduced is via reducing sulphur deposition to zero, and then nitrogen deposition to $CL_{max}N$. In Region 2, a combination of non-zero reductions in sulphur and nitrogen deposition could be used to reduce exceedances. Region 3 exceedances can also be reduced by a combination of sulphur and nitrogen deposition reductions, though as the location of exceedance point E3 approaches the boundary with Region 4, more of the deposition reductions must come from sulphur deposition. In Region 4, reductions in nitrogen deposition will have no effect on exceedances; deposition reductions in sulphur must take place in order to prevent exceedances from occurring. The Regions thus denote different strategies that must be taken to prevent critical load exceedances.

Figure S1. SMB Critical Load Function for acidification, showing exceedance regions 1 through 4 and "below exceedance" region 0. Deposition in exceedance of critical loads correspond to regions 1 through 4, while the grey region encompasses deposition below critical loads. The change in sulphur and nitrogen deposition required to bring a given ecosystem in exceedance to below exceedance is described by ExS, ExN, and the amount in exceedance is the dotted line linking E_i to Z_i. After CLRTAP, 2023, Figure 7.3.

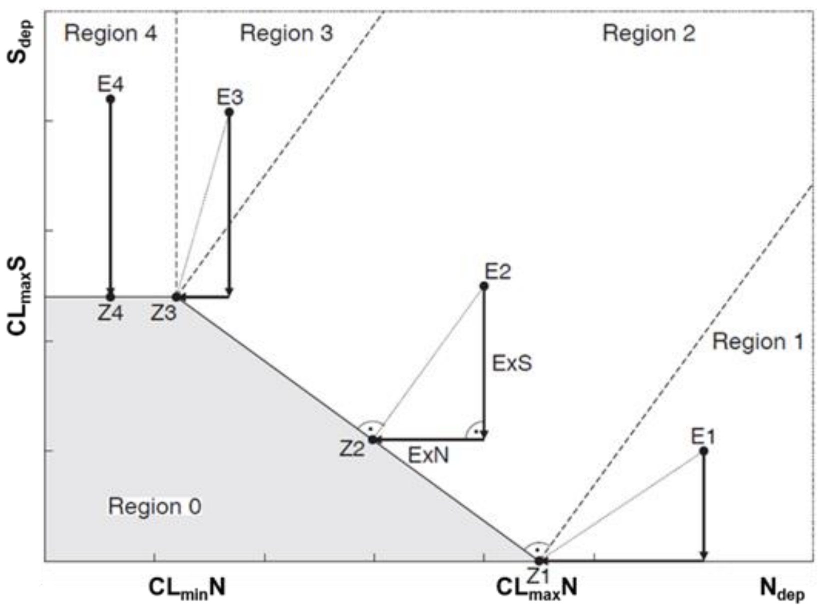

Table S1: Data sources, model types and major parameters for North American forest soil critical loads maps. A database of maps within the U.S.A was provided in National Atmospheric Deposition Program (NADP, 2022). Table adapted from Lynch *et al.* (2022).

Source	**Model**	**Resolution**	**Extent**	**Chemical criteria**	**BC_w approach**	**Uptake**
McNulty *et al.* (2007, 2013)	SMB	1 km^2	U.S.A-wide	Bc/Al, Coniferous forest: 1, deciduous forest: 10	Clay correlation - substrate method	Bc_u, N_u
Duarte *et al.*, (2013)	SMB	5 km^2	New England	Bc/Al = 10	Clay correlation - substrate method	Bc_u, N_u
Phelan *et al.*, (2014; 2016)	SMB	1 m^2	Pennsylvania	Bc/Al =10	PROFILE	Bc_u, N_u
Sullivan *et al.*, (2011, 2012)	MAGIC	Watershed	Virginia and New York	Bc/Al, Ca/Al = 1 and 10, Bsat = 5 and 10	MAGIC	Bc_u
Cathcart *et al.* (2024)	SMB	250 m x 250 m	Canada-wide	Bc/Al = site specific	Soil texture approximation	Bc_u, N_u

S1.2 North America: Aquatic Ecosystems Acidity Critical Loads

The North American Aquatic Ecosystem acidity critical load dataset constructed here combined individual datasets from the Canada and the USA.

S1.2.1 Canada: Aquatic Ecosystem Data

Environment and Climate Change Canada data corresponding to the subset of 2,997 lake surveys which reside within the common AQMEII4 North American grid were used in conjunction with the Steady-State Water Chemistry (SSWC) critical load model (Sverdrup *et al.,* 1990) as described in Aherne and Jeffries

(2015). The SSWC model has been widely used in regional lake critical load assessments across Europe (e.g. Posch *et al.,* 2001), Canada (e.g. Cathcart *et al.,* 2016; Henriksen *et al.,* 2002; Jeffries *et al.,* 2010; Scott *et al.,* 2010; Whitfield *et al.,* 2006; Williston *et al.,* 2016), and the United States (e.g. Dupont *et al.,* 2005; Miller, 2011). Briefly, the critical load exceedance is defined as the difference between the total sulphur deposition S_{dep} and the acidity critical load value CL(A). The latter is determined from the non-marine, pre-acidification base cation flux ($[BC^*]_0$) minus the Acid Neutralizing Capacity limit (ANC_{limit})for protecting aquatic biota from damage, scaled by the catchment runoff (Q):

$$CL(A) = Q([BC^*]_0 - ANC_{limit}) \quad (5)$$

Where available, a site-specific modelled isotope mass balance estimate of Q (Gibson *et al.,* 2010) was used (n=684) in preference to a Q value derived from a GIS-modelled map approach using regional datasets (Reinds *et al.,* 2015). When Dissolved Organic Carbon (DOC, mgC L^{-1}) values were available (n=2,875) the organic acid adjusted ANC_{limit} ($[ANC]_{oaa}$) was used to include the influence of organic acids in the lake as 1/3 the charge density (m, here set to 10.2 μeq mgC^{-1}) (Lydersen *et al.,* 2004; Hruska *et al.,* 2001),

$$[ANC]_{oaa} = [ANC]_{limit} - \frac{m}{3} DOC \quad (6)$$

Where the lake acid neutralizing capacity $[ANC]_{limit}$ is defined as the excess equivalents of cations – anions in lakewater (note that all quantities in these equations are in units of charge equivalents; number of moles multiplied by the charge of the ion, so by convention, charges are not included in the variable names in the exceedance formulae):

$$[ANC]_{limit} = BC_{le} + NH_{4_{le}} - SO_{4_{le}} - NO_{3_{le}} - Cl_{le} \quad (7)$$

BC_{le}, $NH_{4_{le}}$, $SO_{4_{le}}$, $NO_{3_{le}}$, Cl_{le} are the charge equivalents (μeq L^{-1}) of ionic base cations, ammonium, sulphate, nitrate, and chloride in lakewater.

For lakes lacking DOC samples, an ANC_{limit} of 40 μeq L^{-1} was chosen as a conservative value, previously used in regional Canadian assessments (e.g. Henriksen *et al.,* 2002), and based on the response of brown trout (Lien *et al.,* 1996). Since the SSWC model does not consider non-acidifying nitrogen, only sulphur was used to determine exceedance (i.e. exceedance is defined as the total S deposition minus the critical load of Equation (5)).

1.2.2 USA: Aquatic Ecosystem Data

Aquatic critical loads for the USA were taken from the National Critical Loads Database Version 3.2.1 (NCLDv3.2.1, Lynch *et al.,* 2022), which contains both the critical load data used here and supporting information. A total of 21,667 critical loads were used for 14,334 unique lakes and streams across the USA (a combination of different methods for determining the critical loads were included in the USA values, sometimes resulting in more than one CL estimate for the same water body). Most critical loads (78%) were determined using the SSWC model as described above and by equations 5 and 7 (Lynch *et al.,* 2022; Scheffe *et al.,* 2014; Dupont *et al.,* 2005, Miller 2011, VDEC (2003, 2004, 2012)). Site-specific catchment Q estimates for these values were based on 30-year Normals that are included as a catchment parameter in the National Hydrography Dataset Plus (NHD+2, US EPA, 2023). The other 22% of critical loads were determined by a dynamic modelling approach (e.g., MAGIC and PnET-BGC models) (Sullivan *et al.,* 2005; Fakhraei *et al.,* 2014; Lawrence *et al.,* 2015) and a combination of dynamic modeling with a regionalization approach (e.g. hurdle/regional regression modeling) to determine the critical load across the landscape (McDonnell *et al.,* 2012, 2014; Sullivan *et al.,* 2012; and McDonnell *et al.,* 2021). Site-specific catchment Q estimates were also used; these were based on the specific research project. An ANC_{limit} of 50 μeq L^{-1} was used for the Eastern USA, with the exception of streams in the Adirondacks Mountain, NY, which used 20 μeq L^{-1} (McDonnell *et al.* 2021) and 20 μeq L^{-1} for the western USA. Organic acid-adjusted ANC_{limit} values were not used in generating the USA CL(A) datasets. In many cases, multiple studies estimated CL(A) for the same lake or stream, leading to multiple CL(A) estimates for a single water body. An average critical load value was therefore used for these waterbodies with more than one critical load. A more detailed description of the USA aquatic critical loads used here can be found in Lynch *et al.,* (2022).

S1.3 USA: Sensitive Epiphytic Lichen

Critical loads for sensitive epiphytic lichen species richness made use of 9,000 community surveys across the USA from 1990-2012 (Geiser *et al.* 2019), where a 90% quantile regression was used to model relationships between deposition levels and observed species richness in order to estimate critical loads. Here, Geiser *et al.* (2019) sets a -20% decline in species richness (their "Low ecological risk" critical load) as the level of ecosystem damage that can occur before the loss of species impacts the presence of plentiful forage, nesting materials or insect habitat; hence determining the critical load. The models show that there is a consistent relative response of lichen communities across climates, which results in a single critical load of 3.1 kg-N ha^{-1} yr^{-1} for sensitive epiphytic lichen, which can be applied across all ecosystems in which the lichen can be found. This value was applied to all broadleaf, conifer, or mixed forest landcover types as designated by the National Land Cover Database (NLCD, Dewitz 2021). The original 30m resolution NLCD dataset was aggregated to a 240m resolution grid including all cells with greater than 10% forest cover. Exceedances of the above critical load were calculated for each 240m resolution cell based on the annual deposition of the overlapping 0.125° resolution AQMEII4 CTM model cell.

S1.4 USA Herbaceous Plants

The USA herbaceous plants dataset uses the critical load of total nitrogen for a decline in herbaceous species community richness, developed using over 14,000 vegetation survey plots across nitrogen deposition gradients (Simkin *et al.,* 2016). An observation-based approach using median quantile regressions for herbaceous species richness response to deposition was employed, to generate critical loads with respect to nitrogen deposition linked to various atmospheric and soil conditions. A first model was developed for open canopy ecosystems where the critical load varies with observed soil pH, precipitation, and mean temperature. A second model was developed for closed canopy ecosystems where the critical load varies with observed soil pH alone. The plant level critical loads were mapped across the continental U.S. using land cover from the NLCD. Open canopy systems were defined as the combination of the NLCD grassland and shrubland landcover types, while closed canopy ecosystems were defined as the combination of the NLCD's broadleaf, conifer, or mixed forest landcover classes. The resulting critical loads were aggregated to a 240m grid including all cells with greater than 10% cover. Using the United States Department of Agriculture gridded National Soil Survey Geographic Database (gNATSGO) soil pH dataset (https://www.nrcs.usda.gov/resources/data-and-reports/gridded-national-soil-survey-geographic-database-gnatsgo, last access July 12, 2024), and Parameter-elevation Relationships on Independent Slopes Model (PRISM) interpolation data for temperature and precipitation (Daly *et al.*, 2008), the CL of N for open canopy systems ranged from 6.2 to 12.3 kg-N $ha^{-1}yr^{-1}$ and the CLs of N for closed canopy systems ranged from 6.1 to 23.7 kg-N $ha^{-1}yr^{-1}$. The two datasets were then merged into a single CL raster using the minimum CL when cells overlapped. Exceedances of the resulting critical loads for nitrogen deposition were then generated using the annual deposition of the overlapping 0.125° resolution AQMEII4 CTM model cell.

S1.5 EU: Acidification of Terrestrial Ecosystems

The critical load database and the exceedance calculation for Europe were provided by the Coordination Centre for Effects (CCE) under the United Nations Economic Commission for Europe Convention on Long-range Transboundary Air Pollution (UNECE LRTAP Convention), hosted by the Umweltbundesamt (UBA) in Germany, which develops and maintains the European critical loads database (Geupel *et al.*, 2022). The most recent database available was used here and was also used within the review process of the Gothenburg protocol. It typically contains critical load values for acidification and eutrophication, and has two different components. The first component is data delivered by the member countries of the International Cooperative Programme on Modelling and Mapping. This data is collected within an officiated "Call for Data" (CfD) process within the framework of the Working Group on Effects (WGE). The most recent CfD was finalized in the year 2021. The methods used to determine acidification loads are country-dependent, but all make use of the Simple Mass Balance as described above (Sverdrup & De Vries, 1994; CLRTAP, 2023). The country-specific detailed methods and participating countries may be found in Geupel *et al.* (2022). If countries do not deliver their own CL data, the CCE fills these data gaps with its own background database (Reinds *et al.*, 2021).

The decision of the chemical criterion used to define exceedance (e.g., critical aluminium concentration, critical pH, and critical base saturation) and the chosen critical limit value is usually country-specific. The background CCE database makes use of a fixed value based on a critical pH value of 4.2.

S1.6 EU: Eutrophication of Terrestrial Ecosystems

Critical loads for EU eutrophication ($CL_{nut}N$) are also based on the SMB method applied to nitrogen deposition – (Equation 8). Generally, the methods to derive the parameters of this equation are similar for national datasets and the CCE dataset (e.g. the estimation of the nitrogen uptake (N_u) is linked to growth potential of the vegetation, the fraction of the nitrogen which is denitrified (f_{de}) is connected to the soil type). One major difference occurs when it comes to the derivation of the accepted nitrogen leaching ($N_{le(acc)}$) term. There are two ways to estimate the $N_{le(acc)}$. One way is to simply assign how much nitrogen is allowed to leave the ecosystem based on observations. Another way is to calculate the $N_{le(acc)}$ by using the amount of soil runoff (Q) and multiply it with a critical limit for nitrogen concentration. The latter limits can be linked to negative effects for the related ecosystems (such as fine root damage). The choice of the values for the critical limit for nitrogen is one of the main sources for differences in the modelled EC SMB eutrophication CL (see also CLRTAP, 2023). Another main source for differences in the CL values between countries is the integration of so-called empirical critical loads. These empirical values can be used as upper and lower boundaries for the SMB modelling results in order to avoid rather extreme results in ecosystems where the SMB model predicts very high or very low eutrophication CL values. Empirical CL were updated recently and are well documented in Bobbink *et al.* (2022).

$$CL_{nut}N = N_i + N_u + \left(\frac{N_{le\,(acc)}}{1-f_{de}}\right) \quad (8)$$

The CL exceedance was calculated for every available critical load value in the integrated CL database of the CCE (about 4 million EU data points) and later aggregated on the basis of the AQMEII4 deposition grid cells. The resulting EU CLE are summarized as the share of the receptor area with critical load exceedance (bar charts) and the magnitude of the exceedance within each analysis grid cell (maps). The exceedance in a grid cell is defined as the so-called 'average accumulated exceedance' (AAE), which is calculated as the area-weighted average of the exceedances of the critical loads of all ecosystems in this grid cell. The units for critical loads and their exceedances are equivalents per hectare and year, making S and N deposition comparable on their impacts, which is important for acidity CLs.

S1.7 References, Critical Load Exceedances

Aherne, J., and Jeffries, D.: Critical Load Assessments and Dynamic Applications for Lakes in North America. In W. de Vries, J.-P. Hettelingh, and Posch, M. (Eds.): Critical Loads and Dynamic Risk Assessments: Nitrogen, Acidity and Metals in Terrestrial and Aquatic Ecosystems (pp. 485–503). Springer Netherlands., https://doi.org/10.1007/978-94-017-9508-1_19, 2015.

Bobbink, R., Loran, C., and Tomassen, H.: Review and revision of empirical critical loads of nitrogen for Europe. Dessau-Roßlau, UBA TEXTE 02/2022, 2022.

Cathcart, H., Aherne, J., Moran, M.D., Savic-Jovcic, V., Makar, P.A., and Cole, A.: Estimates of critical loads and exceedances of acidity and nutrient nitrogen for mineral soils in Canada for 2014–2016 average annual sulphur and nitrogen atmospheric deposition, EGUsphere [preprint], https://doi.org/10.5194/egusphere-2024-2371, (accepted, November 2024), 2024

Cathcart, H., Aherne, J., Jeffries, D. S., and Scott, K. A.: Critical loads of acidity for 90,000 lakes in northern Saskatchewan: A novel approach for mapping regional sensitivity to acidic deposition. *Atm. Env.*, *146*, 290–299, https://doi.org/10.1016/j.atmosenv.2016.08.048 , 2016.

CLRTAP, 2023: UNECE CLRTAP Manual on Methodologies and Criteria for Modelling and Mapping Critical Loads and Levels and Air Pollution Effects, Risks, and Trends. Dessau-Roßlau, UBA TEXTE 109/2023, https://www.umweltbundesamt.de/en/publikationen/manual-on-methodologies-criteria-for-modelling-0 , 2023.

Daly, C., Halbleib, M., Smith, J.I., Gibson, W.P., Doggett, M.K., Taylor, G.H., Curtis, J., and Pasteris, P.P.: Physiographically sensitive mapping of climatological temperature and precipitation across the conterminous United States, In.t J. Climatol., 2031-2064, 2008.

Dewitz, J.: National Land Cover Database (NLCD) 2019 Products (ver. 2.0, June 2021). U.S. Geological Survey. https://doi.org/10.5066/P9KZCM54, 2021.

Duarte, N., Pardo, L.H., and Robin-Abbott, M.J.: Susceptibility of forests in the northeastern USA to nitrogen and sulfur deposition: critical load exceedance and forest health, Water Air Soil Pollution, 22:1355, 21pp https://link.springer.com/article/10.1007/s11270-012-1355-6 , 2013.

Dupont, J., Clair, T. A., Gagnon, C., Jeffries, D. S., Kahl, J. S., Nelson, S. J., and Peckenham, J. M.: Estimation of Critical Loads of Acidity for Lakes in Northeastern United States and Eastern Canada. *Environmental Monitoring and Assessment*, *109*(1–3), 275–292, https://doi.org/10.1007/s10661-005-6286-x, 2005.

Fakhraei, H.A., Driscoll, C.T., Selvendiran, P., DePinto, J.V., Bloomfield, J., Quinn, S. and Rowell, H.C.: Development of a total maximum daily load (TMDL) for acid-impaired lakes in the Adirondack region of New York, Atm. Env., 95, 277-287, https://doi.org/10.1016/j.atmosenv.2014.06.039, 2014

Geiser, L. H., Nelson, P.R., Jovan, S.E., Root, H.T., and Clark, C.M.: Assessing Ecological Risks from Atmospheric Deposition of Nitrogen and Sulfur to US Forests Using Epiphytic Macrolichens, Diversity 11(6): 87, https://doi.org/10.3390/d11060087, 2019.

Geupel, M., Loran, C., Scheuschner, T., and Wohlgemuth, L.: CCE Status Report. Dessau-Roßlau, UBA TEXTE 135/2022, https://www.umweltbundesamt.de/en/publikationen/cce-status-report-2022, last accessed December 21, 2023, 2022.

Gibson, J. J., Birks, J. S., Jeffries, D. S., Kumar, S., Scott, K. A., Aherne, J., and Shaw, P. D.: Site-specific estimates of water yield applied in regional acid sensitivity surveys across western Canada. *Journal of Limnology*, *69*(1s), 67, https://doi.org/10.4081/jlimnol.2010.s1.67 , 2010.

Henriksen, A., Dillon, P. J., and Aherne, J.: *Critical loads of acidity for surface waters in south-central Ontario, Canada: Regional application of the Steady-State Water Chemistry (SSWC) model*, Can. J. Fish. Aquat. Sci, *59*, 9, https://doi.org/10.1139/f02-092, 2002.

Hruska, J., Köhler, S., Laudon, H., and Bishop, K.: Comparison of acid/base character of organic acids in boreal zone of Sweden and mountainous regions in the Czech Republic. Water Air Soil Pollut (S4-2), p. 100 (in: *Acid Raing 2000, Proceedings from the 6th International Conference on Acid*

Deposition, Kenichi Satake, Ed.), https://link.springer.com/book/10.1007/978-94-007-0810-5, 2001.

Jeffries, D. S., Semkin, R. G., Gibson, J. J., and Wong, I.: Recently surveyed lakes in northern Manitoba and Saskatchewan, Canada: Characteristics and critical loads of acidity. *Journal of Limnology*, *69*(1s), 45, https://doi.org/10.4081/jlimnol.2010.s1.45, 2010.

Lawrence, G. B., T. J. Sullivan, D. A. Burns, S. W. Bailey, B. J. Cosby, M. Dovciak, H. A. Ewing, T. C. McDonnell, R. Minocha, R. Riemann, J. Quant, K. C. Rice, J. Siemion, and Weathers, K.: Acidic deposition along the Appalachian Trail corridor and its effects on acid-sensitive terrestrial and aquatic resources: Results of the Appalachian Trail MEGA-transect atmospheric deposition effects study. Natural Resource Report NPS/NRSS/ARD/NRR—2015/996. National Park Service, Fort Collins, Colorado, https://irma.nps.gov/DataStore/Reference/Profile/2223220, 2015.

Lien, L., Raddum, G. G., Fjellheim, A., and Henriksen, A.: A critical limit for acid neutralizing capacity in Norwegian surface waters, based on new analyses of fish and invertebrate responses. Science of The Total Environment, 177(1–3), 173–193, https://doi.org/10.1016/0048-9697(95)04894-4, 1996.

Liggio, J., Makar, P.A., Li, S-M., Hayden, K., Darlington, A., Moussa, S., Wren, S., Staebler, R., Wentzell, J., Wheeler, M., Leithead, A., Mittermeier, R., Narayan, J., Wolde, M., Blanchard, D., Aherne, J., Kirk, J., Lee, C., Stroud, C., Zhang, J., Akingunola, A., Katal, A., Cheung, P., Ghahreman, R., Majdzadeh, M., He, M., Ditto, J., and Gentner, D.R.: Total organic carbon dry deposition outpaces atmospheric processing with unaccounted implications for air quality and freshwater ecosystems, Science Advances, (accepted), 2024.

Lydersen, E., Larssen, T., and Fjeld, E.: The influence of total organic carbon (TOC) on the relationship between acid neutralizing capacity (ANC) and fish status in Norwegian lakes. *Science of The Total Environment*, *326*(1), 63–69, https://doi.org/10.1016/j.scitotenv.2003.12.005, 2004.

Lynch, J.A., Phelan, J., Pardo, L.H., McDonnell, T.C., Clark, C.M., and Bell, M.D.: Detailed Documentation of the National Critical Load Database (NCLD) for U.S. Critical Loads of Sulfur and Nitrogen, version 3.2.1, National Atmospheric Deposition Program, Wisconsin State Laboratory of Hygiene, Madison, WI., https://nadp.slh.wisc.edu/filelib/claddb/DB_Version/Documentation/NCLD_Documentation_v321.pdf, 2022.

McDonnell, T.C., Driscoll, CT., Sullivan, T.J., Burns, D.A., Baldigo, B.P., Shao, S., and Lawrence, G.B.: Regional target loads of atmospheric nitrogen and sulfur deposition for the protection of stream and watershed soil resources of the Adirondack Mountains, USA. Environmental Pollution 281, 117110, https://doi.org/10.1016/j.envpol.2021.117110, 2021.

McDonnell, T.C., Cosby, B. J., and Sullivan, T. J.,: Regionalization of soil base cation weathering for evaluating stream water acidification in the Appalachian Mountains, USA. Environmental Pollution, 162: 338-344, https://doi.org/10.1016/j.envpol.2011.11.025, 2012.

McDonnell, T.D., Sullivan, T. J., Hessburg, P.F., Reynolds, K.M., Povak, N.A., Cosby, B. J., Jackson, W., and Salter, R.B.: Steady-state sulfur critical loads and exceedances for protection of aquatic ecosystems in the U.S. southern Appalachian Mountains. Journal of Environmental Management 146 (2014) 407-419, 2014. http://dx.doi.org/10.1016/j.jenvman.2014.07.019

Miller, E.: *Steady-state critical loads and exceedances for terrestrial and aquatic eocsystems in the northeastern United States*. Technical report, National Park Service, Air Resources Division, 2011.

McNulty, S. G., Cohen, E. C., and Myers, J. A. M.: Climate change impacts on forest soil critical acid loads and exceedances at a national scale. In: Potter, Kevin M.;Conkling, B. L., Eds. Forest Health Monitoring: National Status, Trends, and Analysis 2010, Gen. Tech. Rep. SRS-GTR-176. Asheville, NC: U.S. Department of Agriculture Forest Service, Southern Research Station. 95-108., 176, 95–108, 2013.

McNulty, S. G., Cohen, E. C., Moore Myers, J. A., Sullivan, T. J., and Li, H.: Estimates of critical acid loads and exceedances for forest soils across the conterminous United States. Environmental Pollution, 149(3), 281–292, https://doi.org/10.1016/j.envpol.2007.05.025, 2007.
Nilsson, J., and Grennfelt, P.: Critical loads for sulphur and nitrogen, in: Report from a workshop held at Skokloster, Sweden 19–24 March 1988, J. Nilsson, Ed., Miljorapport, Volume 15 of Nordic Council of Ministers-Publications-Nord, 418pp, 1988.
Phelan, J.N., Belazid, S., Kurz., D., and Guthrie, S.: Estimation of soil base cation weathering rates with the PROFILE model to determine critical loads of acidity for forested ecosystems in Pennsylvania, USA: pilot application of a potential national methodology, Water Air and Soil Pollution, 225, 2109-2128, https://link.springer.com/article/10.1007/s11270-014-2109-4, 2014.
Phelan, J., Balzid, S., Jones, P., Cajka, J., Buckly, J., and Clark, C.: Assessing the effects of climate change and air pollution on soil properties and plant diversity in sugar maple - beech - yellow birch hardwood forests in the northeastern United States: model simulations from 1900 to 2100, Water Air Soil Pollution, 22:84, 30 pp., https://link.springer.com/article/10.1007/s11270-016-2762-x, 2016.
Posch, M., de Smet, P. A., Hettelingh, J.-P., and Downing, R. J.: *Modelling and mapping of critical thresholds in Europe: Status Report 2001*. Citeseer. https://citeseerx.ist.psu.edu/document?repid=rep1&type=pdf&doi=a585c6eff5f0c93938e4ef21874d4dc9425fd282 , last accessed December 22, 2023, 2001.
Reinds G.J., Thomas D., Posch M., and Slootweg J.: Critical loads for eutrophication and acidification for European terrestrial ecosystems. Final report. Dessau-Roßlau, https://pure.iiasa.ac.at/id/eprint/17341/, 2021.
Reinds, G., Posch, M., Aherne, J.,and Forsius, M.: Assessment of Critical Loads of Sulphur and Nitrogen and Their Exceedances for Terrestrial Ecosystems in the Northern Hemisphere. In: de Vries, W., Hettelingh, JP., and Posch, M. (eds): Critical Loads and Dynamic Risk Assessments. Environmental Pollution, vol 25. Springer, Dordrecht, https://doi.org/10.1007/978-94-017-9508-1_15, 2015.
Scheffe, R. D., Lynch, J. A., Reff, A., Hubbell, B., Greaver, T. L., and Smith, J. T.: The Aquatic Acidification Index: A New Regulatory Metric Linking Atmospheric and Biogeochemical Models to Assess Potential Aquatic Ecosystem Recovery. Water Air Soil Pollution, 225:1838, https://doi.org/10.1007/s11270-013-1838-0, 2014.
Scott, K., Wissel, B., Gibson, J., Birks, S.,: Chemical characteristics and acid sensitivity of boreal headwater lakes in northwest Saskatchewan. *Journal of Limnology*, *69*, 33–44, https://doi.org/10.4081/jlimnol.2010.s1.33, 2010.
Simkin, S. M., Allen, E.B., Bowman, W.D., Clark, C.M., Belnap, J., Brooks, M.L., Cade, B.S., Collins, S.L., Geiser, L.H., Gilliam, F.S., Jovan, S.E., Pardo, L.H., Schulz, B.K., Stevens, C.I., Suding, K.N., Throop, H.L., and Waller, D.M.: Conditional vulnerability of plant diversity to atmospheric nitrogen deposition across the United States, Proc. Nat. Acad. Sci., 113(15), 4086-4091, https://doi.org/10.1073/pnas.1515241113, 2016.
Sullivan, T.J., Cosby, B.J., McDonnell, T.C., Porter, E.M., Blett, T., Haeuber, R., Huber, C.M., and Lynch, J.: Critical loads of acidity to protect and restore acid-sensitive streams in Virginia and West Virginia. Water Air Soil Pollution, 223:5759-5771, https://doi.org/10.1007/s11270-012-1312-4, 2012.
Sullivan, T.J., Cosby, B.J., Driscoll, C.T., McDonnell, T.C., and Herlihy, A.T.: Target loads of atmospheric sulfur deposition to protect terrestrial resources in the Adirondack Mountains, New York against biological impacts caused by soil acidification. J. Environ. Stud. Sci. 1, 301–314, https://pmc.ncbi.nlm.nih.gov/articles/PMC10348011/pdf/nihms-1876861.pdf , 2011.
Sullivan,T.J, Cosby, B.J. Tonnessen, K.A. and Clow, D.W.: Surface water acidification responses and critical loads of sulfur and nitrogen deposition in Loch Vale watershed, Colorado. WATER RESOURCES RESEARCH, VOL. 41, W01021, https://doi.org/10.1029/2004WR003414, 2005.

Sverdrup, H. and de Vries, W.: Calculating critical loads for acidity with the simple mass balance method, Water Air Soil Poll., 72, 143–162, https://doi.org/10.1007/BF01257121, 1994.
Sverdrup, H., De Vries, W., and Henriksen, A.: *Mapping critical loads* (Miljörapport 14). Nordic Council of Ministers, 124pp., https://doi.org/10.1007/BF00283115, 1990.
Sverdrup, H., and Warfvinge, P.: The role of weathering and forestry in determining the acidity of Lakes in Sweden. Water, Air, and Soil Pollution, 52(1), 71–78, 1990.
US EPA, 2023: NHDPlus (National Hydrography Dataset Plus), https://www.epa.gov/waterdata/nhdplus-national-hydrography-dataset-plus , last accessed December 26, 2023.
VDEC, 2003: Vermont Department of Environmental Conservation (VDEC), (2003, 2004, 2012). TOTAL MAXIMUM DAILY LOADS: Acid Impaired Lakes. Watershed Management Division, 103 South Main Street, Building 10 North, Waterbury, VT 05671-0408, 2003, 2004, 2012.
Whitfield, C. J., Aherne, J., Watmough, S. A., Dillon, P. J., and Clair, T. A.: Recovery from acidification in Nova Scotia: Temporal trends and critical loads for 20 headwater lakes. *Canadian Journal of Fisheries and Aquatic Sciences*, *63*(7), 1504–1514, https://doi.org/10.1139/f06-053, 2006.
Williston, P., Aherne, J., Watmough, S., Marmorek, D., Hall, A., de la Cueva Bueno, P., Murray, C., Henolson, A., and Laurence, J. A.: Critical levels and loads and the regulation of industrial emissions in northwest British Columbia, Canada. *Atmospheric Environment*, *146*, 311–323, https://doi.org/10.1016/j.atmosenv.2016.08.058, 2016.

S2.0 Comparison of European Meteorology Anomalies, 2009 versus 2010.

Figure S2 compares temperature and precipitation anomalies for July 2009 to July 2010, relative to the 30 year base period 1961 – 1990 (images and data from the NOAA National Climatic Data Center). July 2010 was significantly hotter (Figure S1(b)) than July 2010 (Figure S1(a)). Precipitation anomalies were relatively similar between July of the two years.

Figure S2. Temperature (a,b) and precipitation (c,d) anomalies relative to the 30-year period 1961-1990, for the years 2009 (a,c) and 2010 (b,d). Note the large positive anomaly (red colours) in temperature for July of 2010 over Europe (b). Data and images from NOAA National Climatic Data Center, https://www.ncei.noaa.gov/access/monitoring/ghcn-gridded-products/maps/, last accessed November 19, 2024.

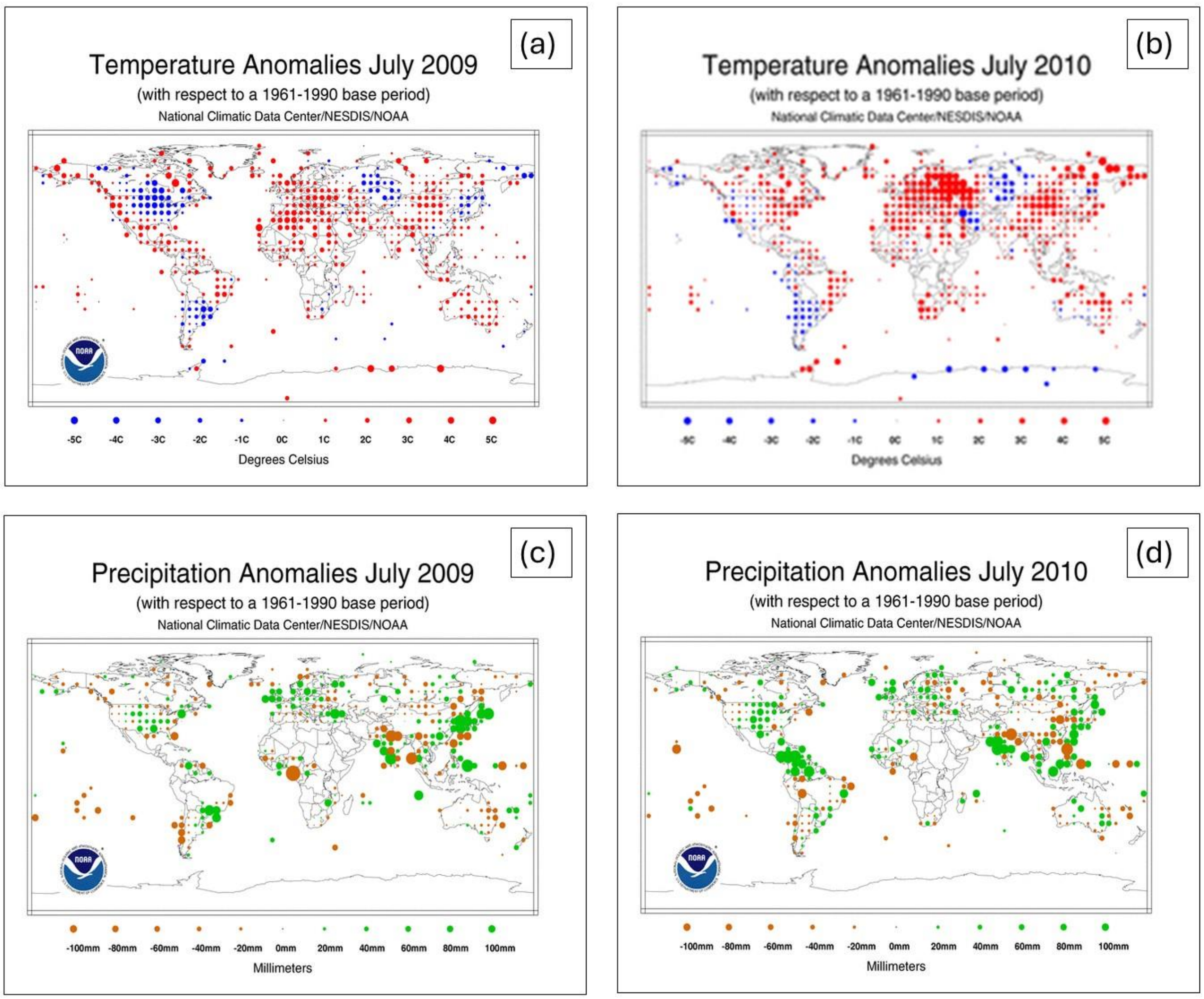

S3.0 Critical Load Exceedance Maps for Europe, 2009, and North America, 2010.

Figure S3. CLEs for Acidity, EU domain, 2009, eq. $ha^{-1}yr^{-1}$ (a) WRF-Chem (IASS), (b) LOTOS-EUROS (TNO), (c) WRF-Chem (UPM), (d) CMAQ (Hertfordshire). Grey areas indicate regions for which critical load data are available but are not in exceedance of critical loads. Coloured areas indicate exceedance regions.

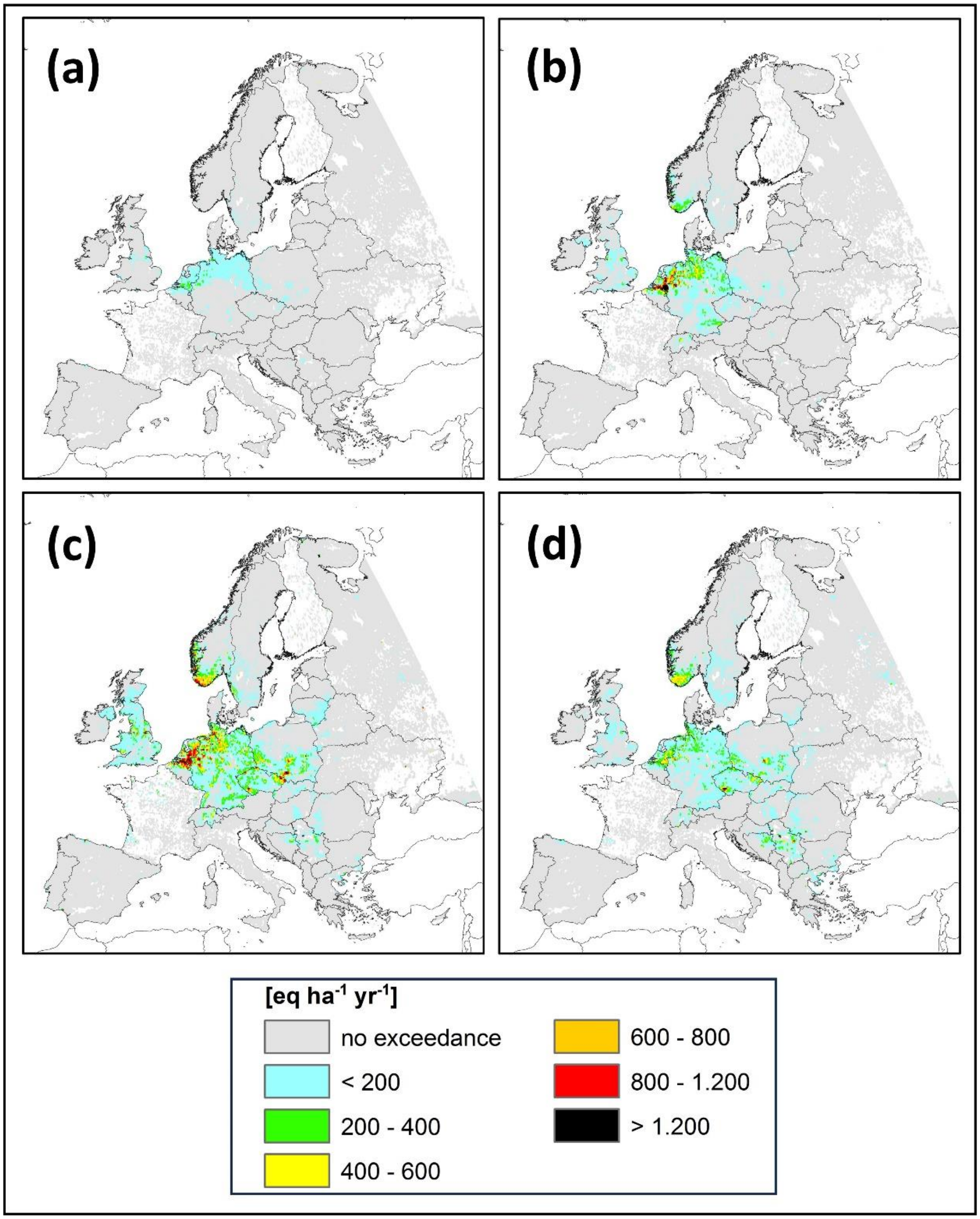

523 Figure S4. CLEs for Eutrophication, EU domain, 2009, eq. $ha^{-1}yr^{-1}$ (a) WRF-Chem (IASS), (b) LOTOS-EUROS (TNO), (c) WRF-Chem (UPM), (d) CMAQ (Hertfordshire). Grey areas indicate regions for which critical load data are available but are not in exceedance of critical loads. Coloured areas indicate exceedance regions.

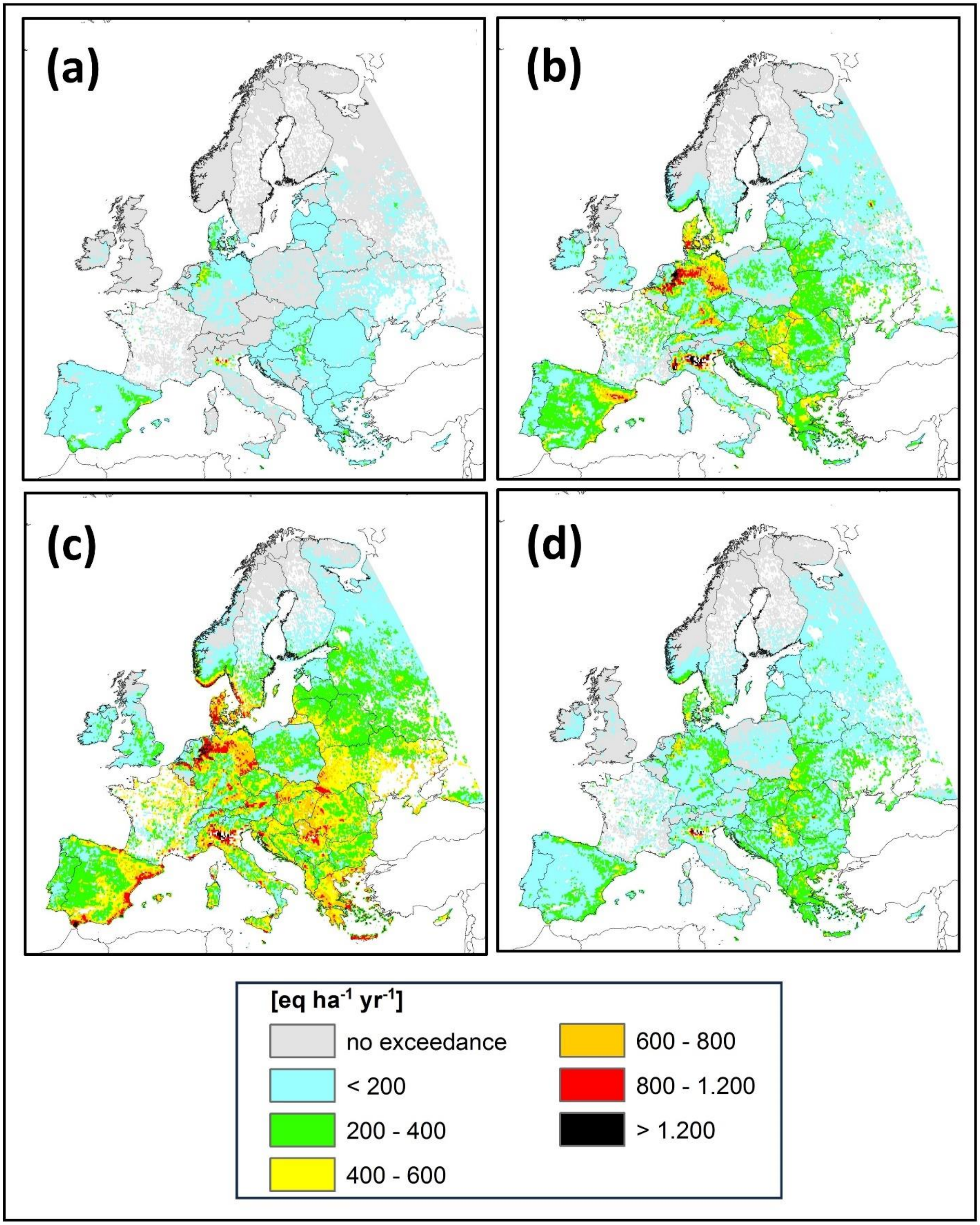

Figure S5. CLEs for Forest Ecosystems, NA domain, 2010, eq. ha^{-1}yr^{-1} (a) CMAQ-M3DRY (EPA), (b) CMAQ-STAGE (EPA), (c) WRF-Chem (IASS), (d) GEM-MACH-Base (ECCC), (e) GEM-MACH-Zhang (ECCC), (f) GEM-MACH-Ops (ECCC), (g) WRF-Chem (UPM), (h) WRF-Chem (UCAR). Grey areas indicate regions for which critical load data are available but are not in exceedance of critical loads. Coloured areas indicate exceedance regions.

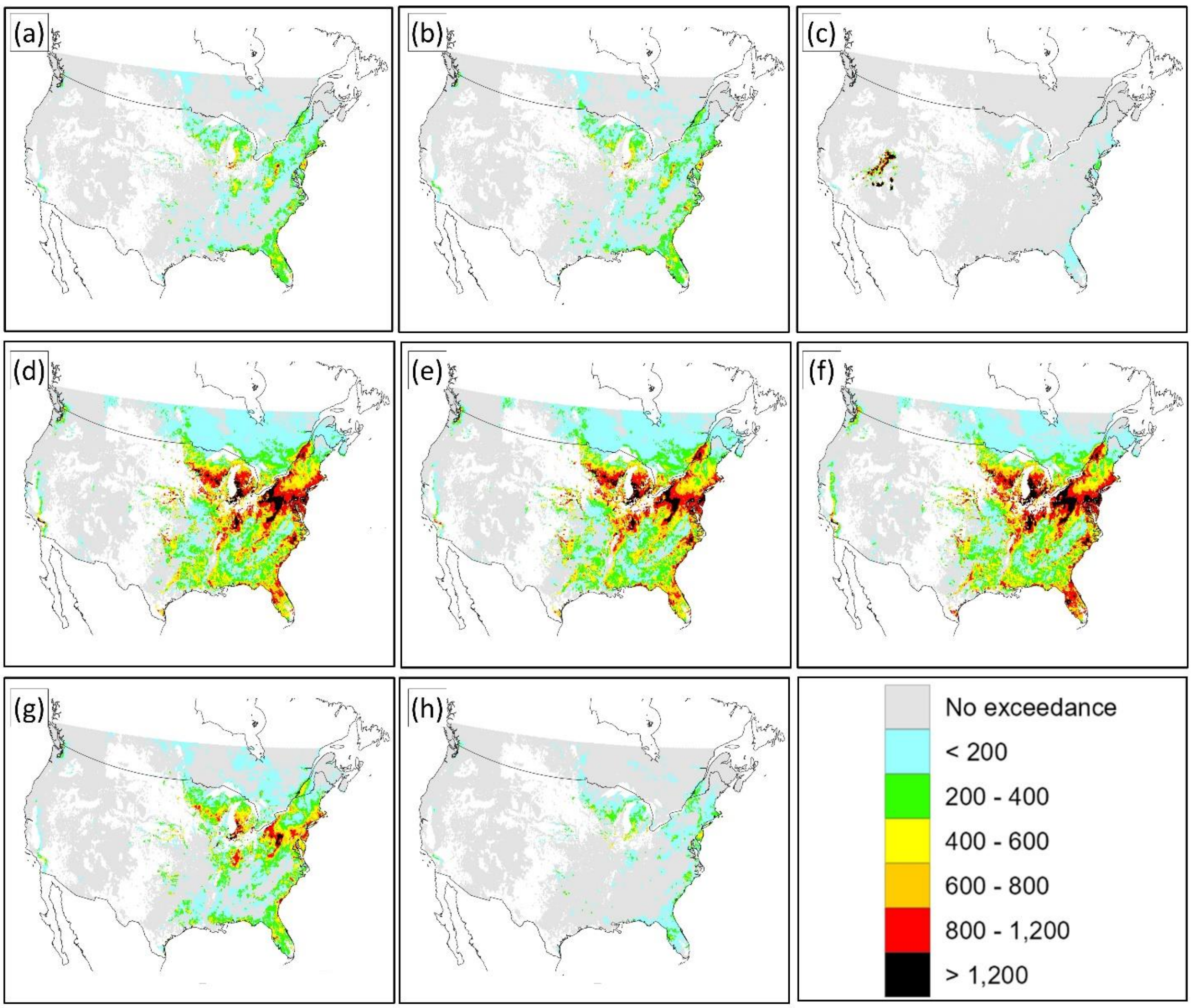

Figure S6. CLEs for Aquatic Ecosystems, NA domain, 2010, eq. $ha^{-1}yr^{-1}$. Panels arranged as in Figure S5; individual lakes are shown as pixels. Light grey pixels indicate regions for which critical load data were available but were not in exceedance of critical loads. Coloured areas indicate exceedance regions; overplotting in precedence by the extent of exceedance was carried out for overlapping pixels.

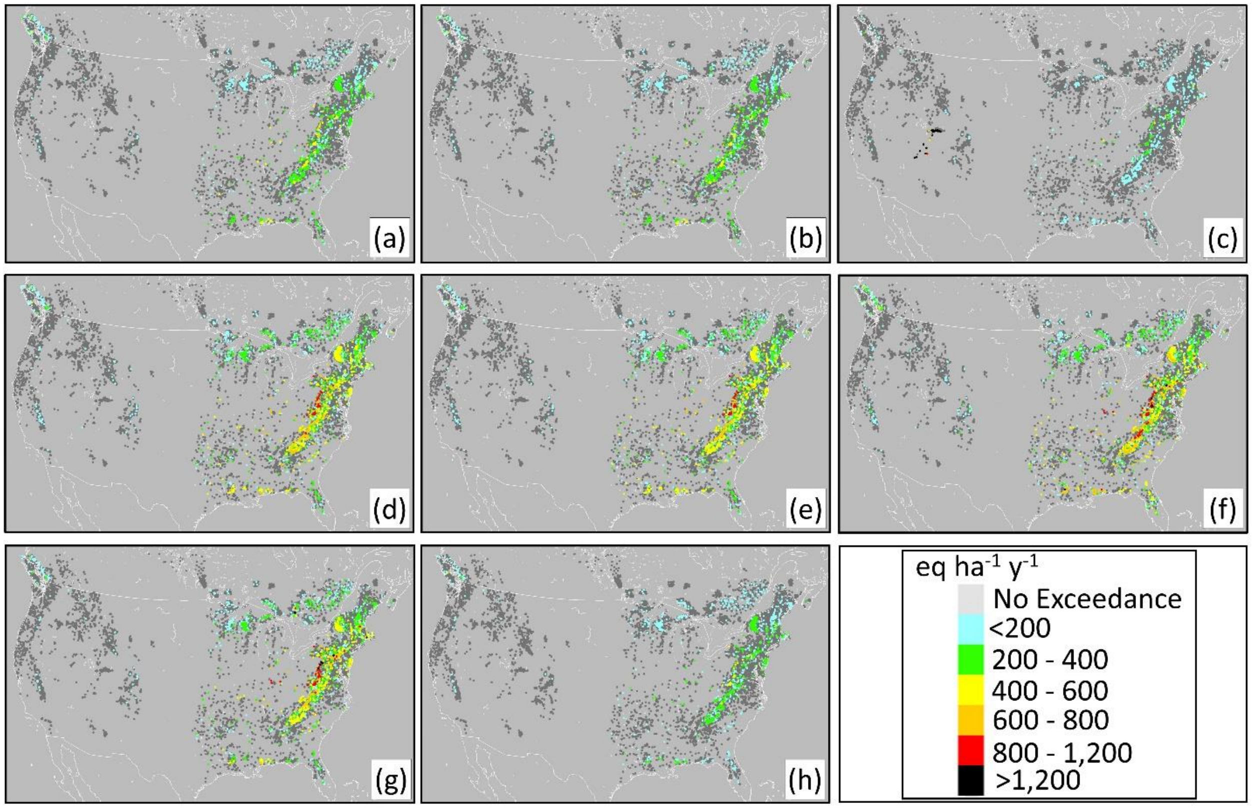

Figure S7. CLEs for Lichen Species, NA domain, 2010, eq. ha^{-1}yr^{-1}. Panels arranged by model as in Figure S5. Light grey areas indicate regions for which critical load data were available but were not in exceedance of critical loads. Coloured areas indicate exceedance regions.

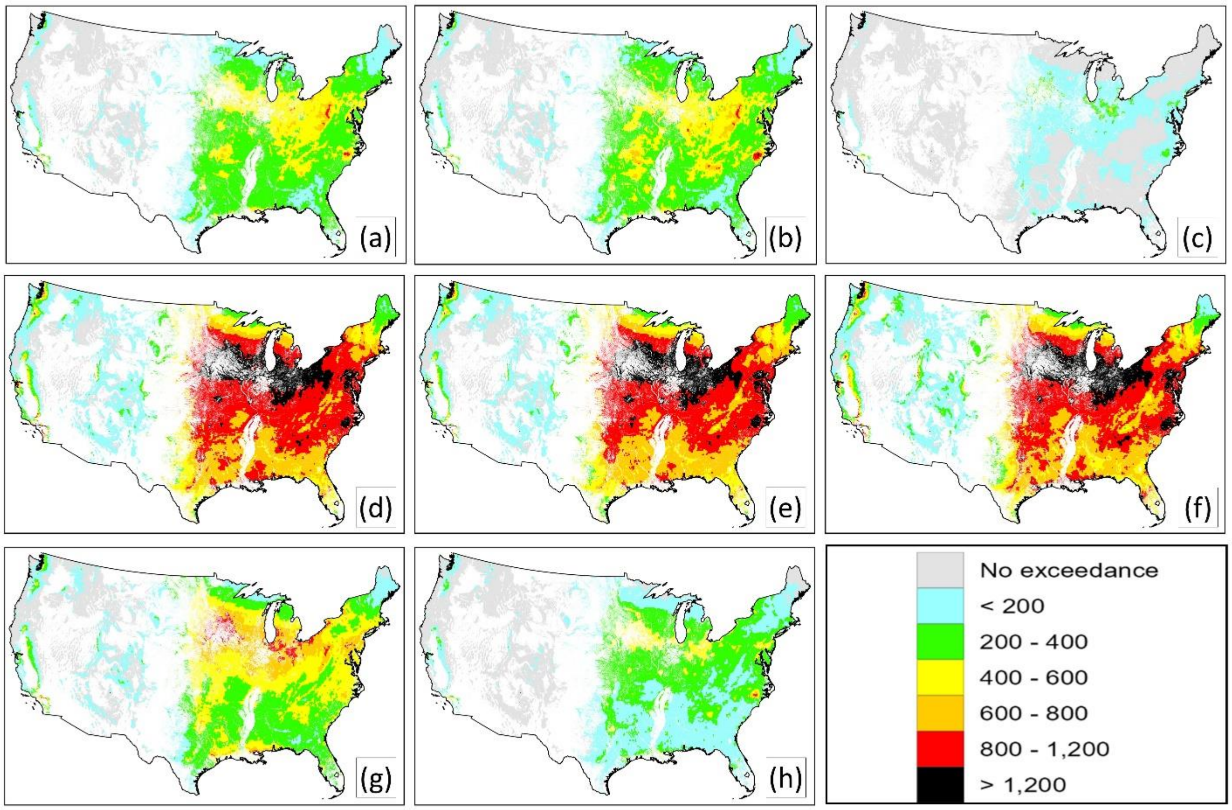

Figure S8. CLEs for Herbaceous Species Community Richness, NA common domain, 2010, eq. ha^{-1}yr^{-1}. Panels arranged by model as in Figure S5. Light grey areas indicate regions for which critical load data were available but were not in exceedance of critical loads. Coloured areas indicate exceedance regions.

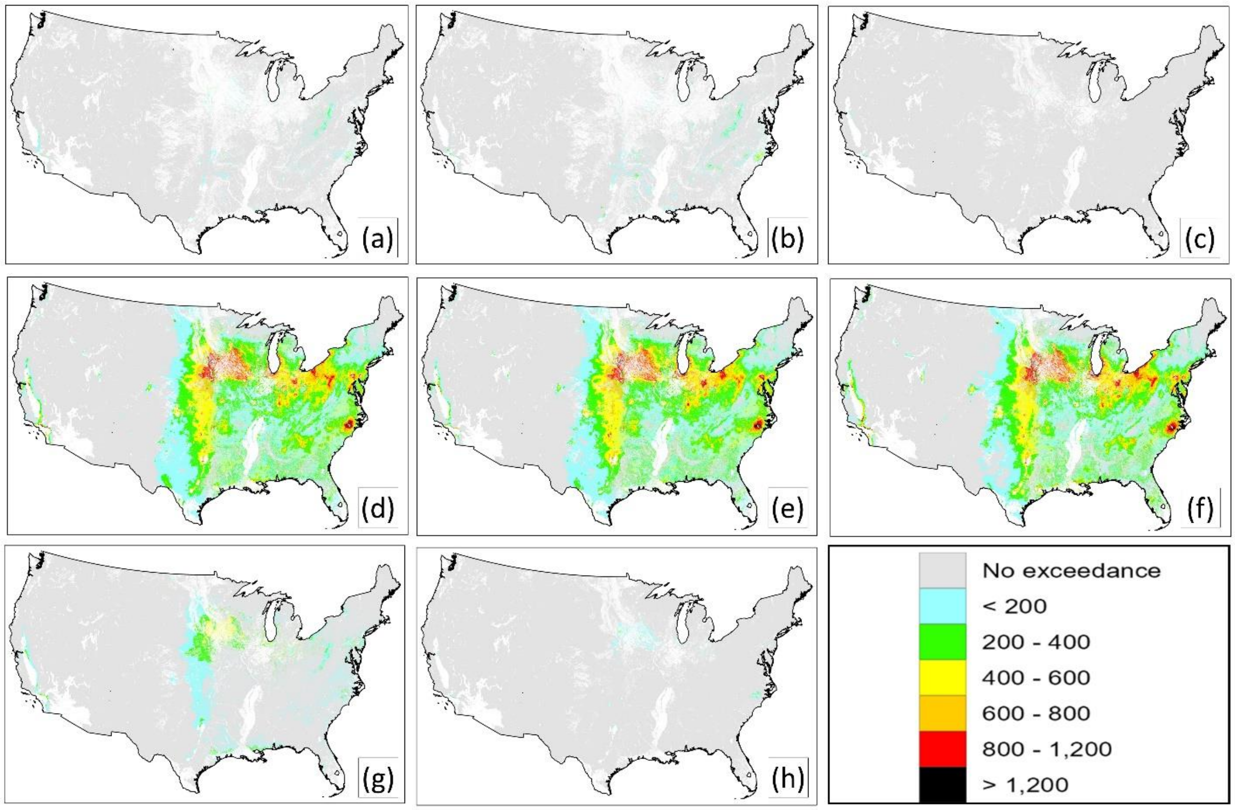

S4.0 Bias-Corrected Critical Load Exceedance Maps for Europe, 2010, and North America, 2016.

Figure S9. Bias-Corrected CLEs for Acidity, EU domain, 2010, eq. $ha^{-1}yr^{-1}$ (a) WRF-Chem (IASS), (b) LOTOS-EUROS (TNO), (c) WRF-Chem (UPM), (d) CMAQ (Hertfordshire). Grey areas indicate regions for which critical load data are available but are not in exceedance of critical loads. Coloured areas indicate exceedance regions.

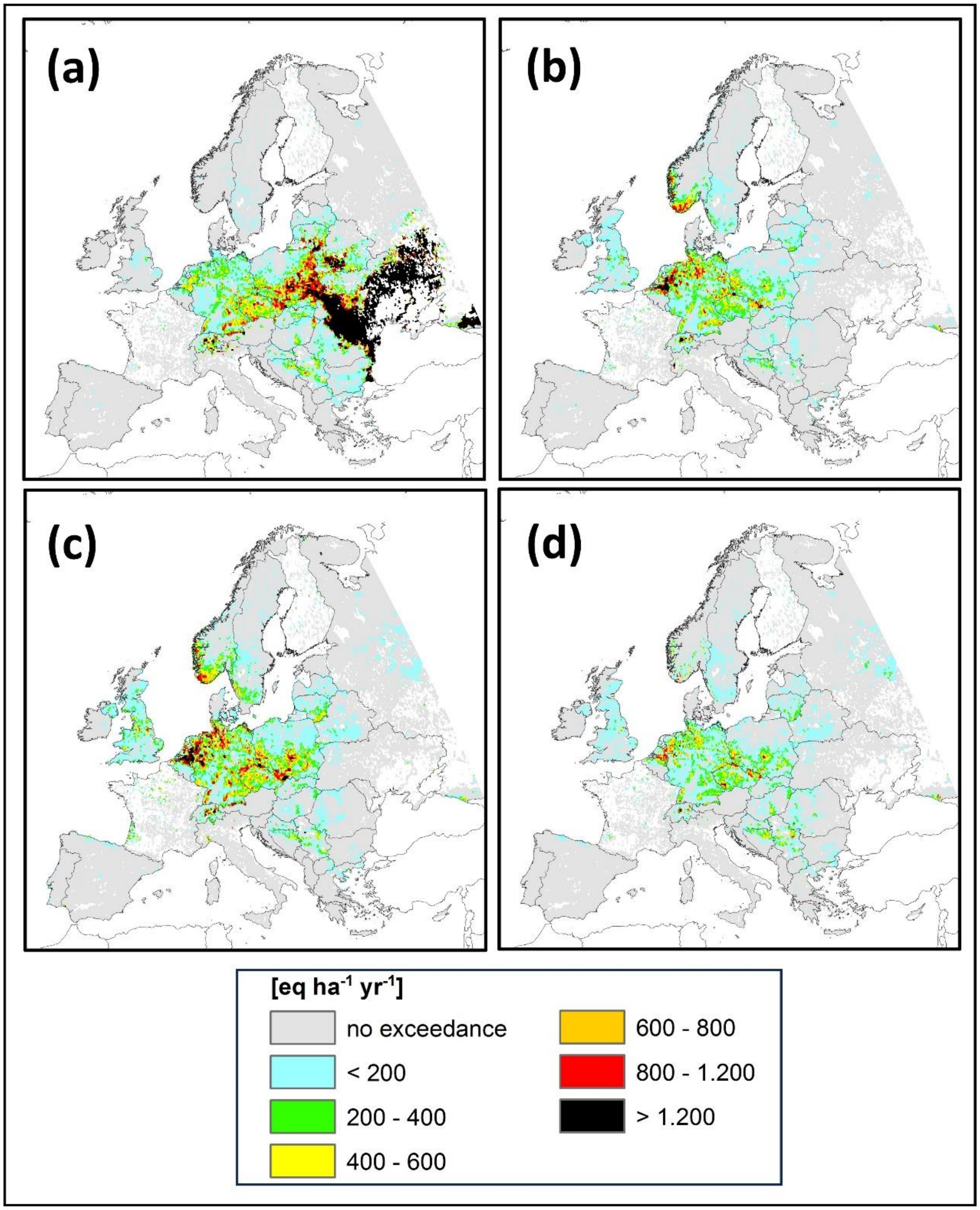

Figure S10. Bias-Corrected CLEs for Eutrophication, EU domain, 2010, eq. $ha^{-1}yr^{-1}$ (a) WRF-Chem (IASS), (b) LOTOS-EUROS (TNO), (c) WRF-Chem (UPM), (d) CMAQ (Hertfordshire). Grey areas indicate regions for which critical load data are available but are not in exceedance of critical loads. Coloured areas indicate exceedance regions.

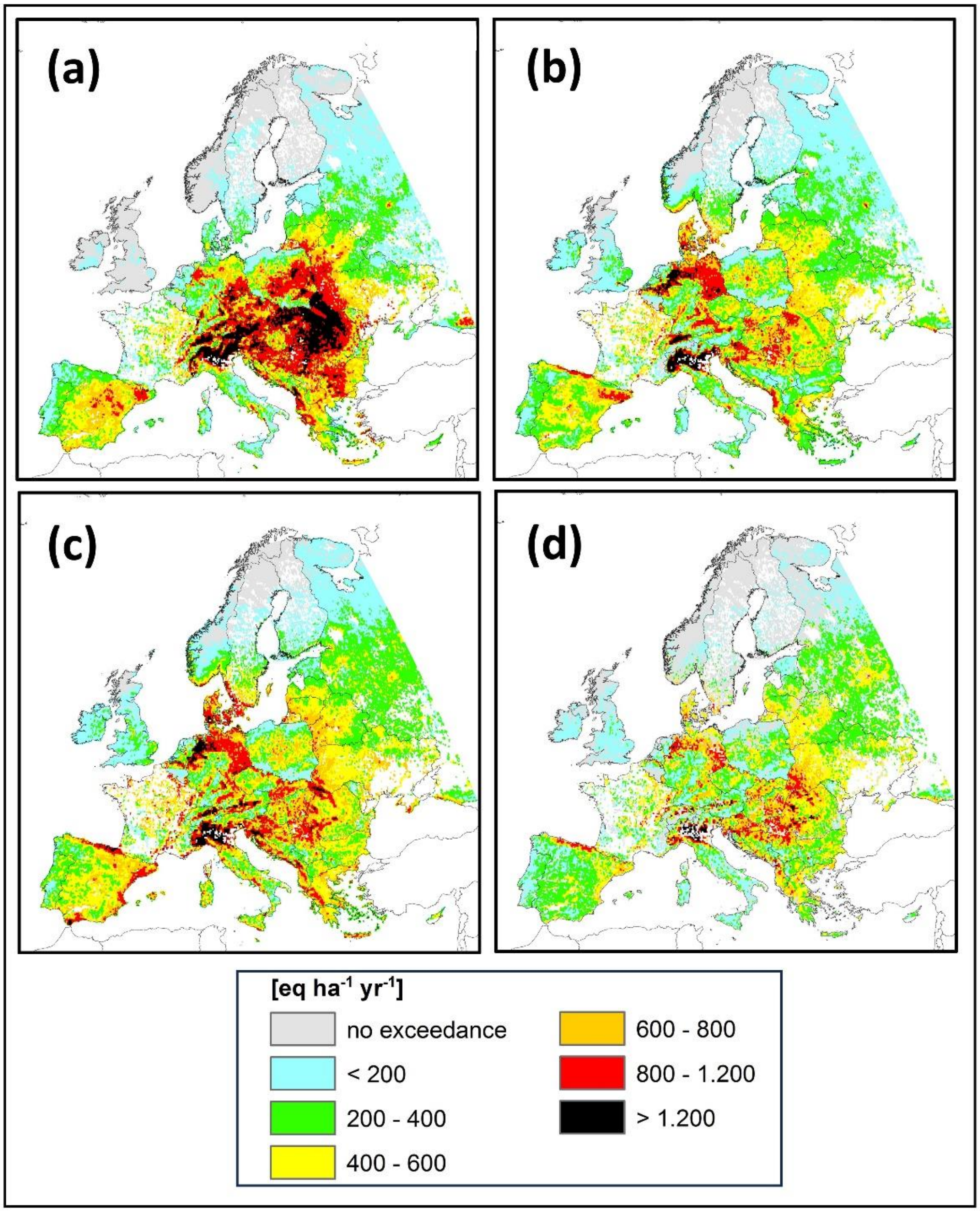

Figure S11. Bias-Corrected CLEs for Forest Ecosystems, NA domain, 2016, eq. ha^{-1}yr^{-1} (a) CMAQ-M3DRY (EPA), (b) CMAQ-STAGE (EPA), (c) WRF-Chem (IASS), (d) GEM-MACH-Base (ECCC), (e) GEM-MACH-Zhang (ECCC), (f) GEM-MACH-Ops (ECCC), (g) WRF-Chem (UPM), (h) WRF-Chem (UCAR). Grey areas indicate regions for which critical load data are available but are not in exceedance of critical loads. Coloured areas indicate exceedance regions.

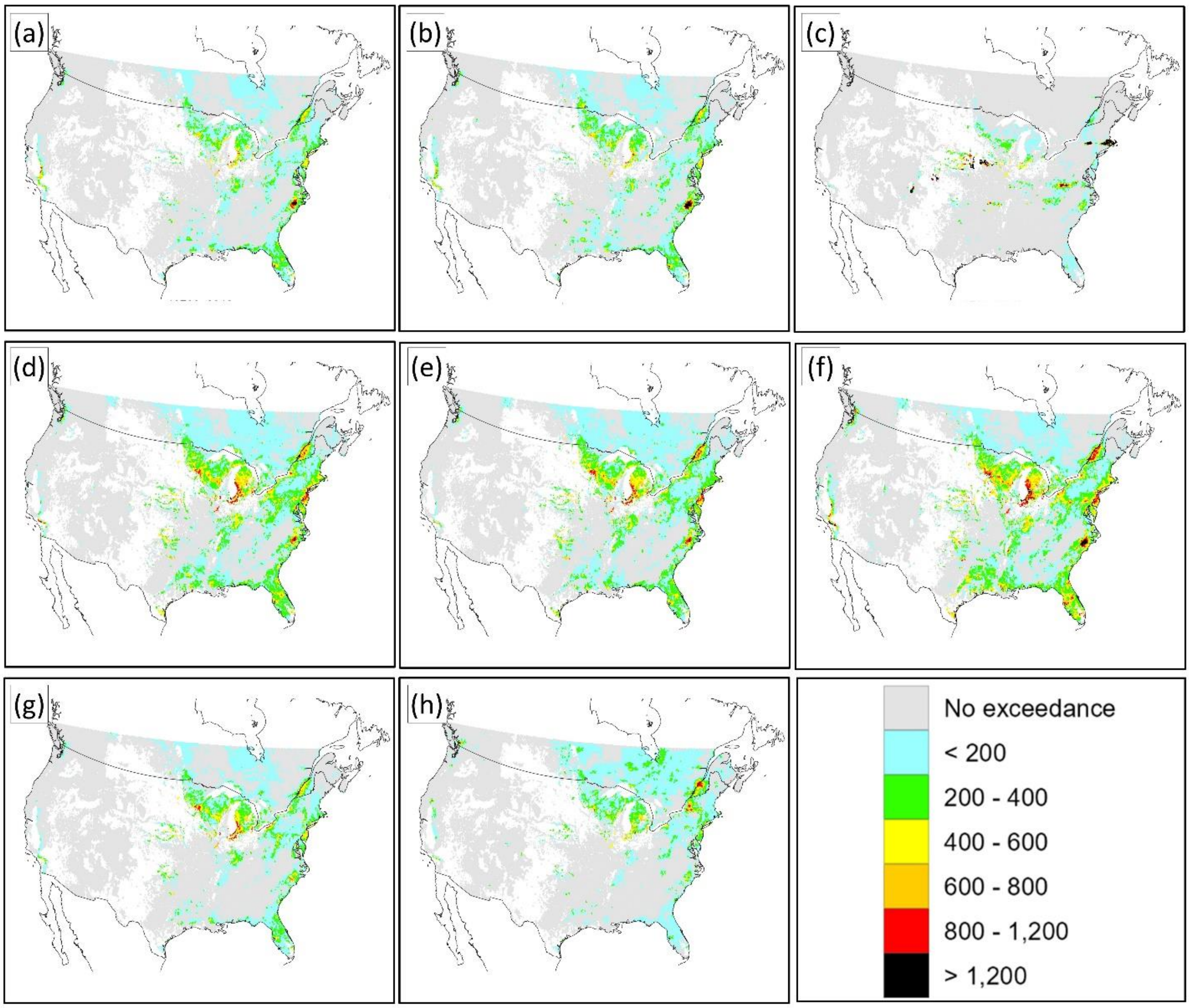

Figure S12. Bias-Corrected CLEs for Aquatic Ecosystems, NA domain, 2016, eq. $ha^{-1}yr^{-1}$. Panels arranged as in Figure S11; individual lakes are shown as pixels. Light grey pixels indicate regions for which critical load data were available but were not in exceedance of critical loads. Coloured areas indicate exceedance regions; overplotting in precedence by the extent of exceedance was carried out for overlapping pixels.

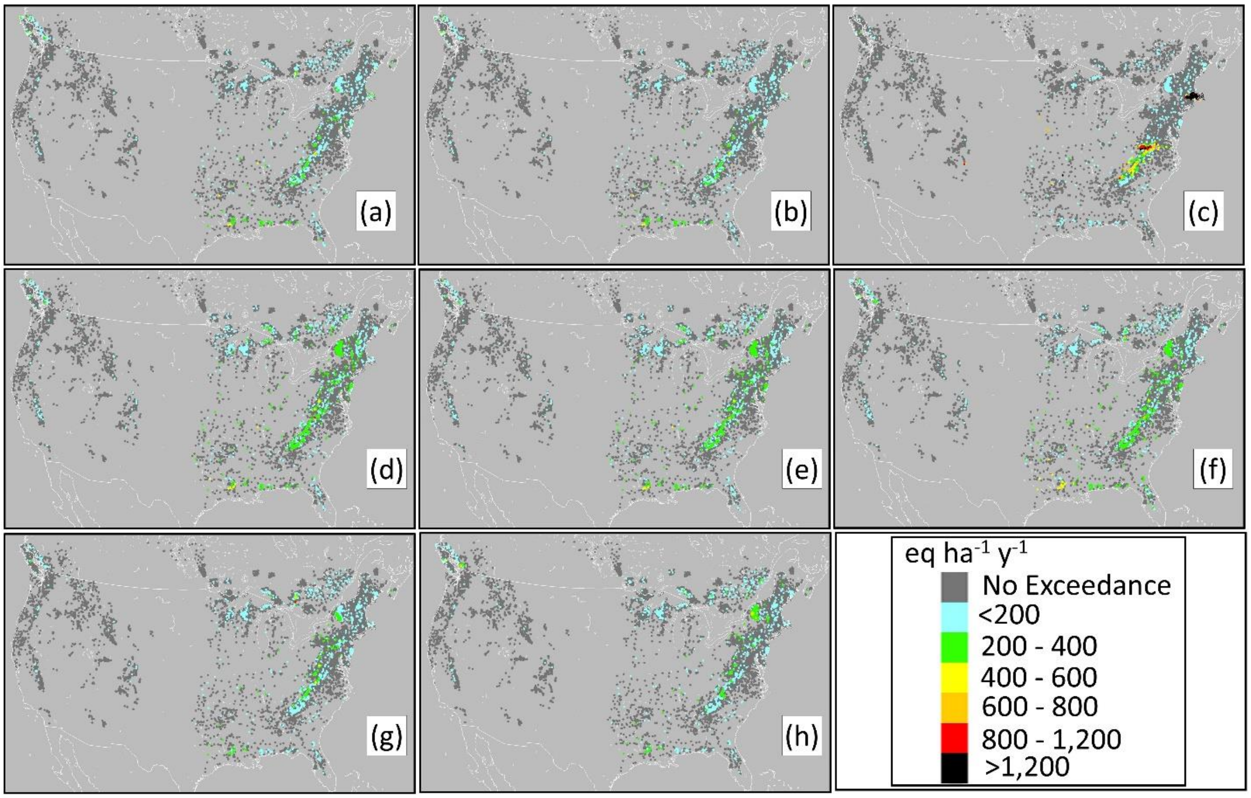

Figure S13. Bias-Corrected CLEs for Lichen Species, NA domain, 2016, eq. ha^{-1}yr^{-1}. Panels arranged by model as in Figure S11. Light grey areas indicate regions for which critical load data were available but were not in exceedance of critical loads. Coloured areas indicate exceedance regions.

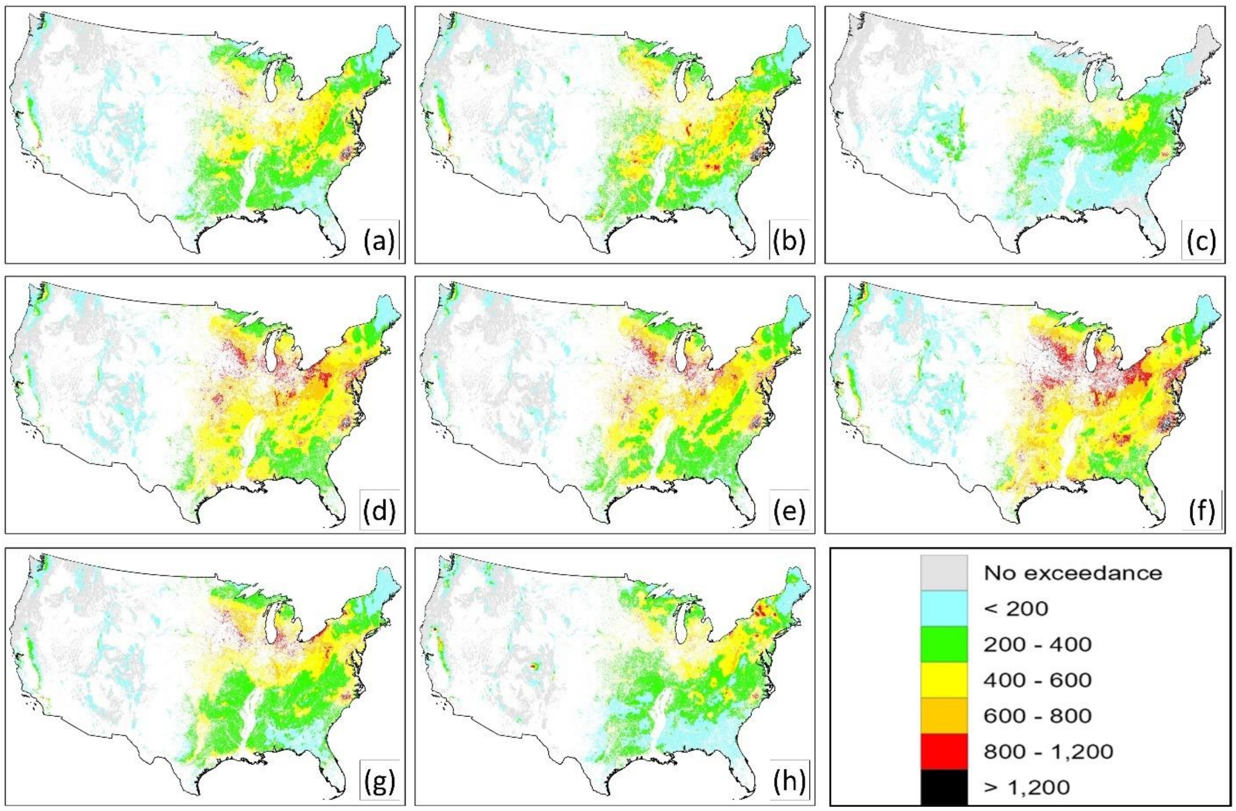

Figure S14. Bias-Corrected CLEs for Herbaceous Species Community Richness, NA common domain, 2016, eq. $ha^{-1}yr^{-1}$. Panels arranged by model as in Figure S11. Light grey areas indicate regions for which critical load data were available but were not in exceedance of critical loads. Coloured areas indicate exceedance regions.

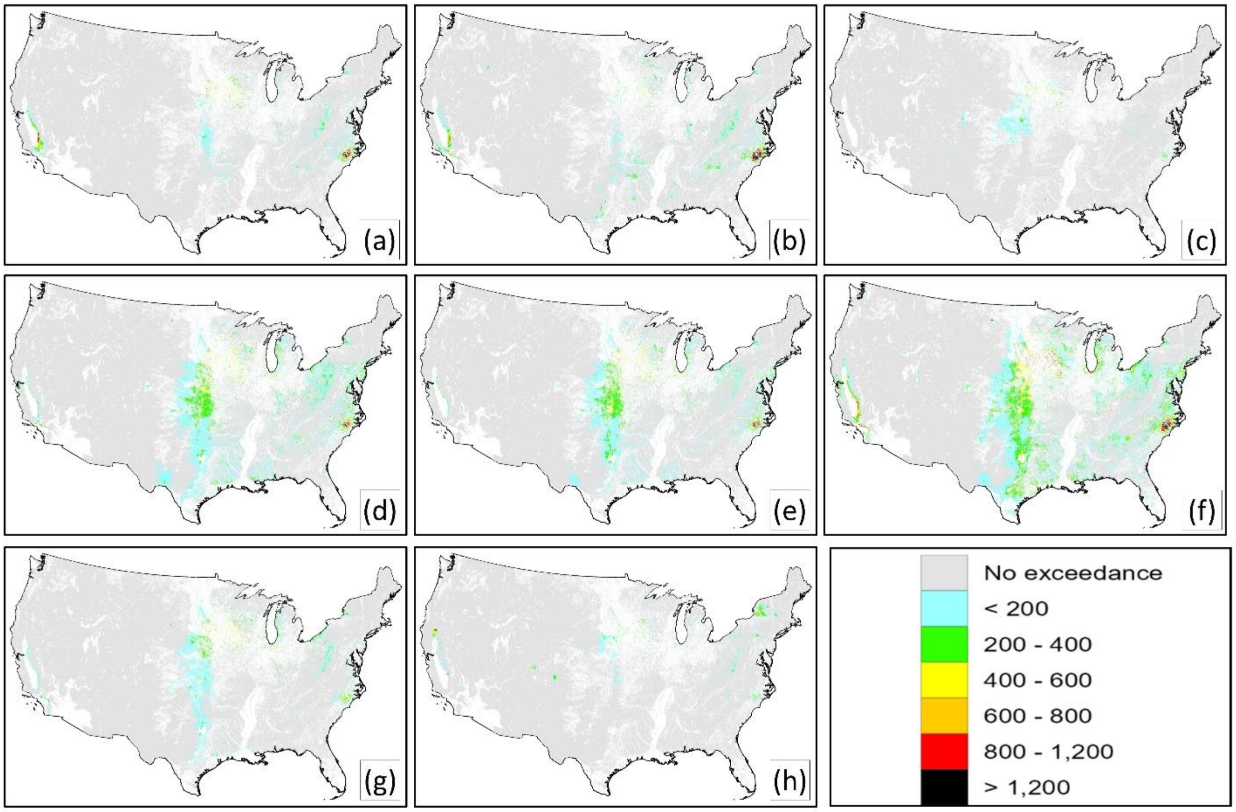

S5.0 Observation Station Locations

Figure S15. Wet deposition and PM2.5 sulphate and ammonium station locations. (a) Wet S deposition station locations (yellow: CAPMoN daily wet deposition; green: NADP weekly wet deposition, (b) Daily PM2.5 sulphate and ammonium air concentration station locations.

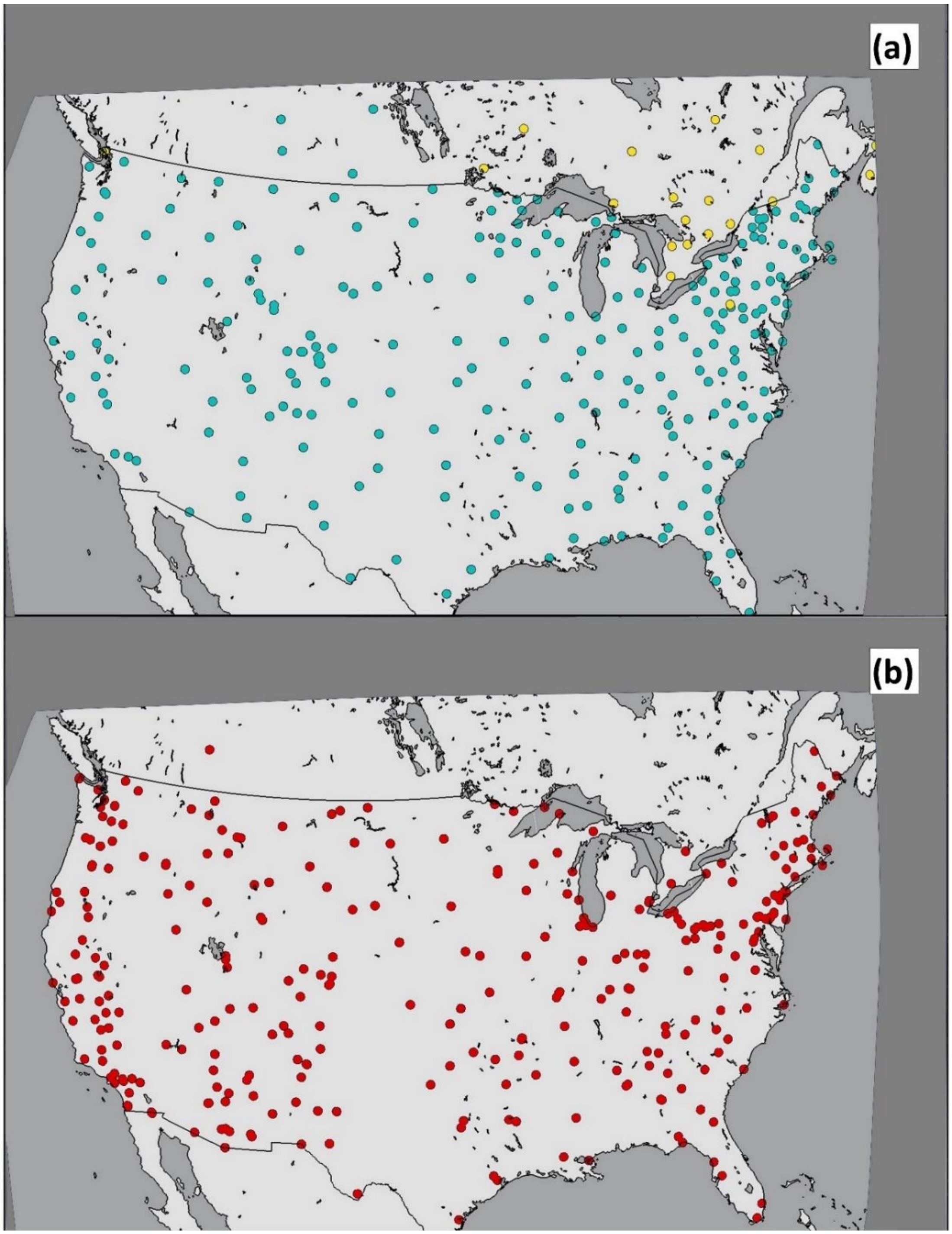

Figure S16. SO2 and AMoN NH3 station locations. (a) SO_2 surface observation station locations (yellow: CAPMoN daily; yellow: NADP hourly green), (b) AMoN NH_3 Observation Stations, 2016.

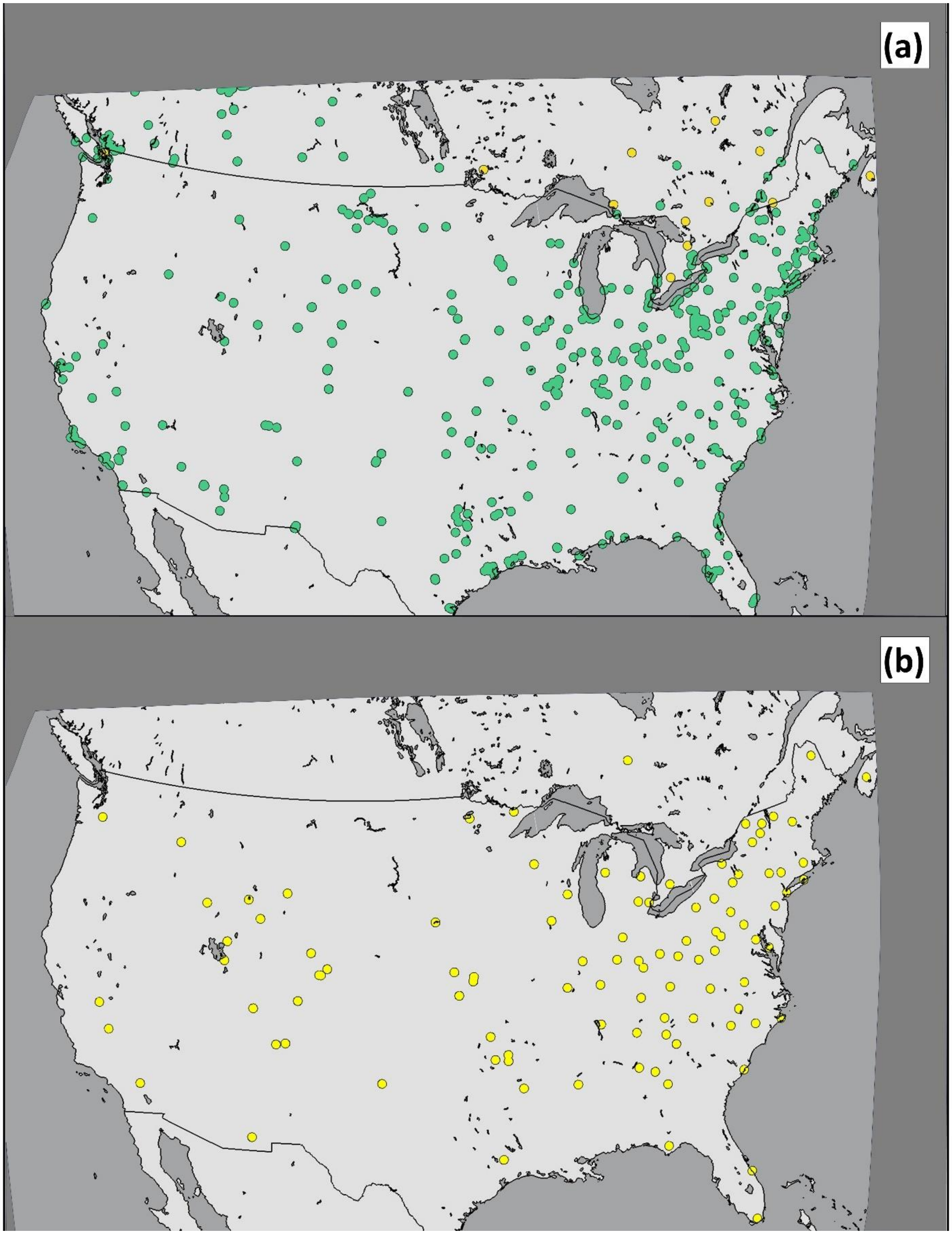

Figure S17. EU SO2 and wet deposition station locations. (a) SO_2 surface observation station locations (yellow: EMEP Hourly; green: AIRBASE hourly), and (b) EMEP wet deposition observation stations, EU AQMEII4 common domain, 2010.

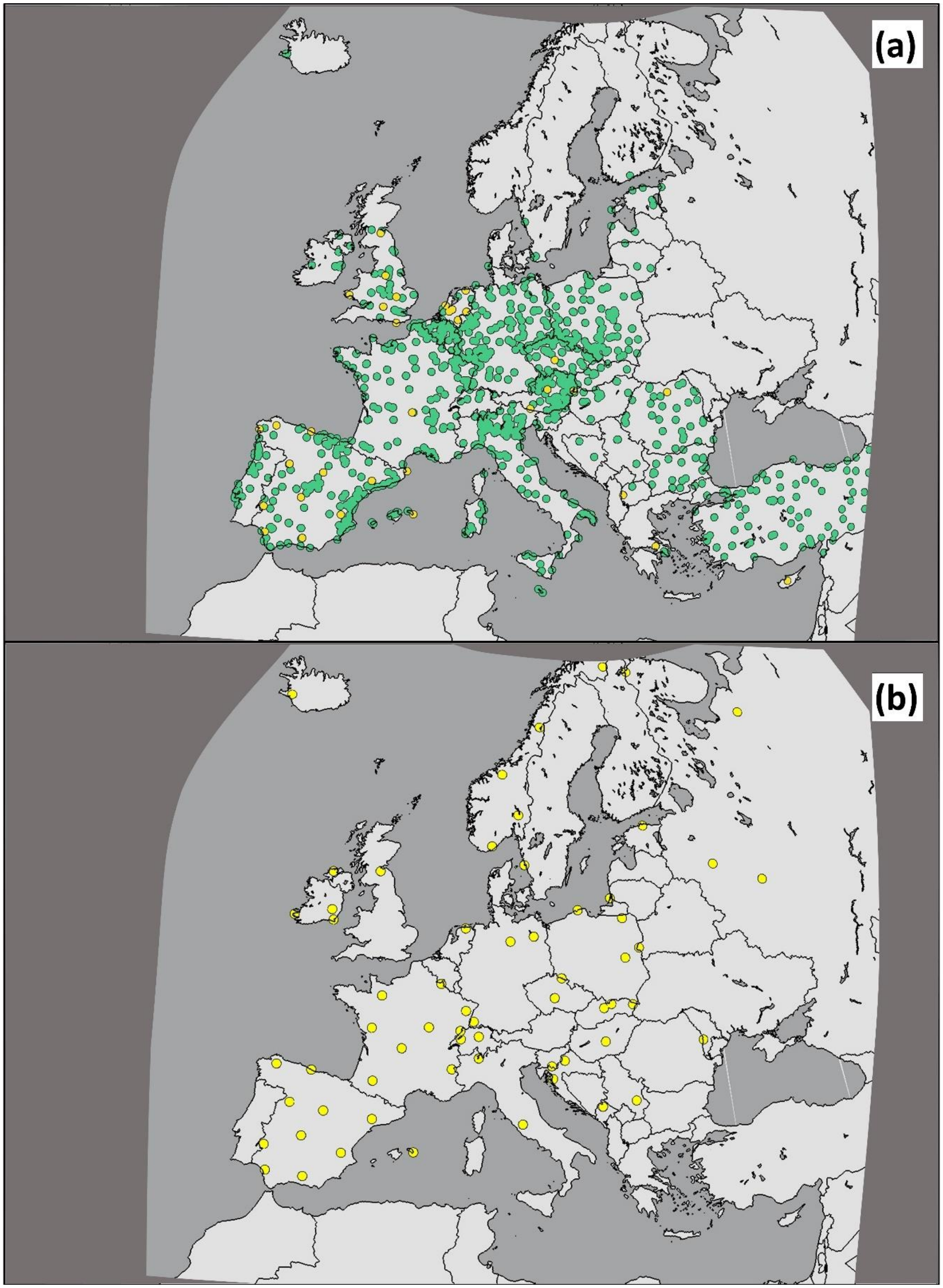

S6.0 Cross-track Infrared Sounding (CrIS) Sensor Retrieval Details

S6.1 Background Information

The satellite surface volume mixing ratio ammonia observations are from the Cross-track Infrared Sounding (CrIS) sensor using the CrIS Fast Physical Retrieval (CFPR) algorithm (Shephard and Cady-Pereira, 2015; Shephard et al., 2020) with updates that include account for non-detects (White et al., 2023). The CrIS instrument pixel footprint is a 14 km circle at nadir with a 2200 km swath that provides complete daily global coverage. The CFPR minimum detection limit can vary depending on the atmospheric state but is as low as ~0.3-0.5 ppbv in favourable retrieval conditions (e.g. Kharol et al., 2018). In this study the CFPR 2016 pixel-level daytime observations, from NOAA/NASA Suomi National Polar-orbiting Partnership (SNPP) satellite over North America with a daytime local solar overpass time of 13:30, were gridded and averaged into annual values with a grid spacing of ~12.5 km to match up with model simulations.

S6.2 References for CrIS retrievals

Kharol, S. K., Shephard, M.W., McLinden, C. A., Zhang, L., Sioris,C. E., O'Brien, J. M., Vet, R., Cady-Pereira, K. E., Hare, E.,Siemons, J., and Krotkov, N. A.: Dry deposition of reactive nitrogen from satellite observations of ammonia and nitrogen dioxide over North America, Geophys. Res. Lett., 45, 1157–1166, https://doi.org/10.1002/2017GL075832, 2018.

Shephard, M. W., and Cady-Pereira, K. E.: Cross-track Infrared Sounder (CrIS) satellite observations of tropospheric ammonia, Atmos. Meas. Tech., 8, 1323–1336, https://doi:10.5194/amt-8-1323-2015, 2015.

Shephard, M. W.; Dammers, E., Cady-Pereira, K. E., Kharol, S. K., Thompson, J., Gainariu-Matz, Y., Zhang, J., McLinden, C. A., Kovachik, A., Moran, M., Bittman, S., Sioris, C., Griffin, D.;, Alvarado, M. J., Lonsdale, C., Savic-Jovcic, V., and Zheng, Q.: Ammonia measurements from space with the Cross-track Infrared Sounder (CrIS): characteristics and applications, Atmos. Chem. Phys., 20, 2277–2302, https://doi.org/10.5194/acp-20-2277-2020, 2020.

White, E., Shephard, M.W., Cady-Pereira, K.E., Kharol, S., Ford, S., Dammers,,E., Chow, E., Thiessen, N., Tobin, D., Quinn, G., O'Brien, J., Bash, J.: Accounting for Non-detects in Satellite Retrievals: Application Using CrIS Ammonia Observations, Remote Sensing, 15, 2610, https://doi.org/10.3390/ rs15102610, 2023.

S7.0 Monitoring Network Statistical Evaluation Tables

Table S2. Model Performance Metrics for SO2, PM2.5 SO4, Wet deposition of S, AQMEII4 North American domain, 2016. Bold-face letters show the highest scoring model.

Hourly SO_2 (units ppbv where applicable)								
Performance Measure	CMAQ-M3Dry	CMAQ-STAGE	WRF-Chem (IASS)	GEM-MACH (Base)	GEM-MACH (Zhang)	GEM-MACH (Ops)	WRF-Chem (UPM)	WRF-Chem (UCAR)
FAC2	0.27	**0.28**	0.26	**0.28**	**0.28**	**0.28**	0.26	0.29
MB	-0.18	-0.17	**-0.03**	0.11	0.14	0.24	0.61	0.17
MGE	**0.91**	**0.91**	1.02	1.08	1.09	1.17	1.43	1.09
NMGE	**1.02**	**1.02**	1.15	1.21	1.22	1.32	1.60	1.22
RMSE	**3.14**	**3.14**	3.29	3.33	3.34	3.51	3.75	3.21
R	**0.15**	**0.15**	0.12	0.14	0.14	0.13	0.13	0.13
COE	**0.04**	0.03	-0.08	-0.14	-0.16	-0.24	-0.51	-0.15
IOA	**0.52**	**0.52**	0.46	0.43	0.42	0.38	0.25	0.43
$PM_{2.5}$ SO_4 (units µg m^{-3}, where applicable)								
FAC2	**0.77**	0.76	0.33	0.65	0.66	0.63	0.67	0.59
MB	-0.04	**0.00**	-0.41	0.28	0.26	0.10	0.10	0.32
MGE	**0.31**	0.32	0.45	0.50	0.50	0.46	0.43	0.55
NMGE	**0.43**	**0.43**	0.60	0.68	0.67	0.62	0.58	0.75
RMSE	**0.89**	**0.89**	1.00	1.10	1.09	1.06	1.00	1.12
R	0.45	**0.46**	0.40	0.40	0.40	0.38	0.39	0.40
COE	**0.37**	0.36	0.10	-0.02	0.00	0.07	0.13	-0.12
IOA	**0.68**	**0.68**	0.55	0.49	0.50	0.54	0.57	0.44
Daily Total Wet S Deposition (units eq. ha^{-1} d^{-1}, where applicable)								
FAC2	0.35	0.36	0.00	0.40	0.40	**0.41**	0.39	0.19
MB	-0.19	-0.17	-0.57	-0.07	-0.08	0.09	**-0.06**	-0.31
MGE	**0.37**	**0.37**	0.57	0.42	0.42	0.48	0.45	0.46
NMGE	**0.65**	**0.65**	1.00	0.74	0.74	0.85	0.79	0.81
RMSE	**0.71**	**0.71**	1.02	0.81	0.81	0.88	0.90	0.89
R	**0.61**	**0.61**	0.06	0.52	0.52	0.54	0.47	0.44
COE	**0.31**	**0.31**	-0.06	0.21	0.22	0.10	0.16	0.14
IOA	**0.65**	**0.65**	0.47	0.60	0.61	0.55	0.58	0.57
Weekly Total Wet S Deposition (units eq. ha^{-1} $week^{-1}$, where applicable)								
FAC2	0.46	**0.47**	0.00	0.41	0.41	0.41	0.45	0.21
MB	-0.21	-0.17	-1.78	-0.41	-0.42	0.30	**-0.03**	-1.18
MGE	**1.12**	**1.12**	1.81	1.18	1.18	1.40	1.28	1.38
NMGE	**0.62**	**0.62**	1.00	0.65	0.66	0.78	0.71	0.76
RMSE	**2.30**	**2.30**	3.26	2.30	2.30	2.54	2.48	2.64
R	**0.63**	**0.63**	0.03	0.55	0.55	0.57	0.53	0.46
COE	**0.34**	**0.34**	-0.07	0.30	0.30	0.17	0.24	0.18
IOA	**0.67**	**0.67**	0.46	0.65	0.65	0.58	0.62	0.59

Table S3. Model Performance Metrics for PM2.5 ammonium, wet deposition of ammonium ion, wet deposition of nitrate ion, AQMEII4 North American domain, 2016. Bold-face letters show the highest scoring model.

$PM_{2.5}$ NH_4 (units μg m^{-3}, where applicable)								
Performance Measure	CMAQ-M3Dry	CMAQ-STAGE	WRF-Chem (IASS)	GEM-MACH (Base)	GEM-MACH (Zhang)	GEM-MACH (Ops)	WRF-Chem (UPM)	WRF-Chem (UCAR)
FAC2	0.48	**0.49**	0.31	0.45	0.42	0.46	0.51	0.46
MB	-0.07	-0.04	**0.03**	0.32	0.41	0.20	0.10	0.06
MGE	**0.23**	0.24	0.33	0.45	0.52	0.38	0.31	0.31
NMGE	**0.68**	0.70	0.96	1.31	1.53	1.10	0.91	0.91
RMSE	**0.59**	0.60	0.75	0.81	0.93	0.75	0.69	0.69
R	**0.37**	**0.37**	0.30	0.33	0.32	0.32	0.30	0.23
COE	**0.19**	0.17	-0.13	-0.55	-0.80	-0.30	-0.08	-0.08
IOA	**0.60**	0.58	0.43	0.23	0.10	0.35	0.46	0.46
Daily Total Wet NH_4 Deposition (units eq. ha^{-1} d^{-1}, where applicable)								
FAC2	0.26	0.29	0.00	0.39	0.38	**0.43**	0.28	0.14
MB	-0.49	-0.44	-0.94	-0.01	**0.00**	-0.10	-0.39	-0.59
MGE	0.67	**0.65**	0.94	0.76	0.78	0.68	0.71	0.80
NMGE	0.72	**0.69**	1.00	0.81	0.83	0.73	0.76	0.86
RMSE	1.46	**1.43**	1.90	1.66	1.71	1.45	1.54	1.73
R	0.55	0.57	0.26	0.52	0.51	**0.59**	0.49	0.37
COE	0.32	**0.34**	0.05	0.23	0.21	0.31	0.28	0.19
IOA	0.66	**0.67**	0.53	0.61	0.61	0.65	0.64	0.59
Weekly Total Wet NH_4 Deposition (units eq. ha^{-1} $week^{-1}$, where applicable)								
FAC2	0.28	0.33	0.00	0.41	0.42	**0.44**	0.31	0.14
MB	-1.51	-1.29	-2.97	0.39	0.38	**0.08**	-1.19	-2.18
MGE	2.13	**2.03**	2.97	2.46	2.44	2.18	2.12	2.43
NMGE	0.72	**0.68**	1.00	0.82	0.82	0.73	0.71	0.82
RMSE	4.29	**4.13**	5.49	5.06	5.02	4.42	4.25	4.78
R	0.50	0.53	0.29	0.51	0.51	**0.54**	0.50	0.40
COE	0.25	**0.28**	-0.05	0.13	0.14	0.23	0.25	0.14
IOA	0.62	**0.64**	0.47	0.57	0.57	0.62	0.63	0.57
Daily Total Wet NO_3 Deposition (units eq. ha^{-1} d^{-1}, where applicable)								
FAC2	0.39	0.39	0.00	0.38	0.39	**0.49**	0.43	0.28
MB	-0.18	-0.16	-0.68	-0.26	-0.19	-0.07	**-0.05**	-0.34
MGE	**0.44**	**0.44**	0.68	0.45	0.46	**0.44**	0.48	0.52
NMGE	0.65	0.65	1.00	0.66	0.68	**0.64**	0.71	0.76
RMSE	**0.80**	**0.80**	1.16	0.84	0.85	0.83	0.89	0.97
R	0.61	**0.62**	0.22	0.56	0.56	0.59	0.55	0.44
COE	0.28	0.28	-0.11	0.27	0.25	**0.29**	0.22	0.15
IOA	**0.64**	**0.64**	0.45	0.63	0.63	**0.64**	0.61	0.58
Weekly Total Wet NO_3 Deposition (units eq. ha^{-1} $week^{-1}$, where applicable)								
FAC2	**0.50**	**0.50**	0.00	0.42	0.45	0.49	0.43	0.33
MB	-0.10	**-0.06**	-1.86	-0.64	-0.41	**0.06**	0.10	-0.87
MGE	**1.09**	**1.09**	1.86	1.12	1.12	1.17	1.34	1.26
NMGE	**0.58**	0.59	1.00	0.60	0.60	0.63	0.72	0.68
RMSE	**1.86**	1.88	2.93	1.96	1.95	1.93	2.23	2.19
R	**0.65**	**0.65**	0.35	0.58	0.58	0.60	0.53	0.48
COE	**0.32**	**0.32**	-0.16	0.30	0.30	0.27	0.16	0.21
IOA	**0.66**	**0.66**	0.42	0.65	0.65	0.64	0.58	0.61

Table S4. Evaluation of model predictions of NH3 against retrieved CrIS NH3 concentrations at overpass time, AQMEII4 common NA grid, 2016. Units ppbv where required.

Evaluation Metric	CMAQ-M3Dry	CMAQ-STAGE	GEM-MACH (Base)	GEM-MACH (Zhang)	GEM-MACH (Ops)	WRF-Chem (UPM)	WRF-Chem (UCAR)
FAC2	0.28	0.38	**0.68**	**0.68**	0.40	0.38	0.58
MB	-0.68	-0.57	**0.09**	**0.09**	-0.54	-0.54	-0.27
MGE	0.83	0.76	0.63	0.63	0.72	0.72	**0.61**
NMGE	0.64	0.58	0.48	0.48	0.55	0.56	**0.47**
RMSE	1.16	1.03	1.07	1.06	1.00	**0.94**	1.00
R	0.66	0.72	0.77	**0.78**	0.70	0.76	0.74
COE	-0.63	-0.50	-0.24	-0.24	-0.41	-0.43	**-0.21**
IOA	0.18	0.25	0.38	0.38	0.29	0.29	**0.40**

Table S5. Evaluation of model predictions of NH3 against annual average AMoN biweekly NH3 concentrations model-observation pairs, 2016. Units ppbv where required.

Evaluation Metric	CMAQ-M3Dry	CMAQ-STAGE	GEM-MACH (Base)	GEM-MACH (Zhang)	GEM-MACH (Ops)	WRF-Chem (UPM)	WRF-Chem (UCAR)
FAC2	0.66	0.62	0.67	0.67	0.72	**0.76**	0.66
MB	-0.82	-0.88	**0.09**	**0.02**	-0.80	-0.61	0.27
MGE	1.24	1.12	1.21	1.18	1.12	**1.08**	1.28
NMGE	0.60	0.54	0.59	0.57	0.54	**0.52**	0.62
RMSE	2.71	2.53	2.72	2.72	2.65	**2.57**	2.95
R	0.37	**0.45**	0.39	0.39	0.39	0.40	0.38
COE	0.21	0.29	0.23	0.25	0.29	**0.32**	0.19
IOA	0.61	0.65	0.61	0.62	0.64	**0.66**	0.59

Table S6. Model performance statistics for EU domain SO2 concentrations and total wet S deposition, μg m^{-3} and eq. ha^{-1} yr^{-1}, respectively.

	SO_2 (Airbase)					SO_2 (EMEP)			
	WRF-Chem (IASS)	LOTOS-EUROS (TNO)	WRF-Chem (UPM)	CMAQ (Hertford shire)		WRF-Chem (IASS)	LOTOS-EUROS (TNO)	WRF-Chem (UPM)	CMAQ (Hertfords hire)
FAC2	0.35	0.36	**0.38**	0.35		0.35	**0.36**	0.34	0.29
MB	-1.42	**0.04**	0.06	1.89		**0.32**	0.48	0.58	1.76
MGE	**4.60**	5.32	5.29	6.35		**1.48**	1.66	1.63	2.57
NMGE	**0.85**	0.98	0.97	1.17		**1.07**	1.20	1.18	1.87
RMSE	**14.47**	15.64	15.27	17.60		**2.92**	3.58	2.98	5.80
R	**0.28**	0.26	0.24	0.26		**0.38**	0.33	0.34	0.35
COE	**0.12**	-0.01	-0.01	-0.21		**-0.08**	-0.21	-0.19	-0.88
IOA	**0.56**	0.49	0.50	0.40		**0.46**	0.40	0.40	0.06

	Total Wet S deposition			
	WRF-Chem (IASS)	LOTOS-EUROS (TNO)	WRF-Chem (UPM)	CMAQ (Hertford shire)
FAC2	0.00	0.19	0.28	**0.31**
MB	-1.51	-1.22	-1.08	**-0.39**
MGE	1.53	1.34	**1.29**	1.42
NMGE	1.00	0.87	**0.84**	0.92
RMSE	6.61	6.50	6.48	**6.46**
R	0.02	0.11	0.11	**0.15**
COE	0.04	0.16	**0.19**	0.11
IOA	0.52	0.58	**0.60**	0.56

Table S7. Model performance statistics for wet deposition of nitrate and ammonium ions, and ground level concentrations of NO_2, AQMEII4 EU domain, 2010

	Wet NO_3^- deposition (eq. ha^{-1} yr^{-1})					Wet NH_4^+ deposition (eq. ha^{-1} yr^{-1})			
	WRF-Chem (IASS)	LOTOS-EUROS (TNO)	WRF-Chem (UPM)	CMAQ (Hertfordshire)		WRF-Chem (IASS)	LOTOS-EUROS (TNO)	WRF-Chem (UPM)	CMAQ (Hertfordshire)
FAC2	0.00	0.32	**0.35**	0.31	FAC2	0.02	**0.32**	0.28	0.24
MB	-1.38	-0.75	**-0.04**	-0.58	MB	-1.80	**-0.80**	-1.01	-1.13
MGE	1.38	**1.04**	1.33	1.11	MGE	1.81	**1.52**	1.55	1.53
NMGE	0.99	**0.75**	0.96	0.80	NMGE	0.98	**0.82**	0.84	0.83
RMSE	2.66	**2.19**	2.53	2.25	RMSE	3.83	**3.37**	3.45	3.42
R	0.16	**0.43**	0.36	0.38	R	0.18	**0.33**	0.32	**0.33**
COE	-0.10	**0.17**	-0.06	0.11	COE	0.00	**0.15**	0.14	**0.15**
IOA	0.45	**0.59**	0.47	0.56	IOA	0.50	**0.58**	0.57	**0.58**
	AIRBASE NO_2 concentrations (µg m^{-3})					EMEP NO_2 concentrations (µg m^{-3})			
	WRF-Chem (IASS)	LOTOS-EUROS (TNO)	WRF-Chem (UPM)	CMAQ (Hertfordshire)		WRF-Chem (IASS)	LOTOS-EUROS (TNO)	WRF-Chem (UPM)	CMAQ (Hertfordshire)
FAC2	0.45	**0.56**	0.55	0.35	FAC2	**0.57**	0.53	0.39	0.50
MB	-10.00	-5.68	**2.38**	-12.40	MB	**0.36**	2.35	9.54	-2.02
MGE	12.67	**11.22**	13.61	13.84	MGE	5.01	6.18	11.49	**4.90**
NMGE	0.60	**0.53**	0.65	0.66	NMGE	0.57	0.70	1.31	**0.56**
RMSE	19.25	**16.76**	19.19	20.41	RMSE	**8.17**	10.01	17.28	8.29
R	0.49	**0.56**	0.47	0.50	R	**0.71**	0.64	0.61	0.67
COE	0.10	**0.20**	0.03	0.02	COE	0.31	0.15	-0.59	**0.32**
IOA	0.55	**0.60**	0.52	0.51	IOA	0.65	0.57	0.21	**0.66**

6.0 Precipitation Evaluation

Figure S18. Precipitation totals expressed as monthly averages, for (a) Daily NADP sites and (b) Weekly CAPMoN sites.

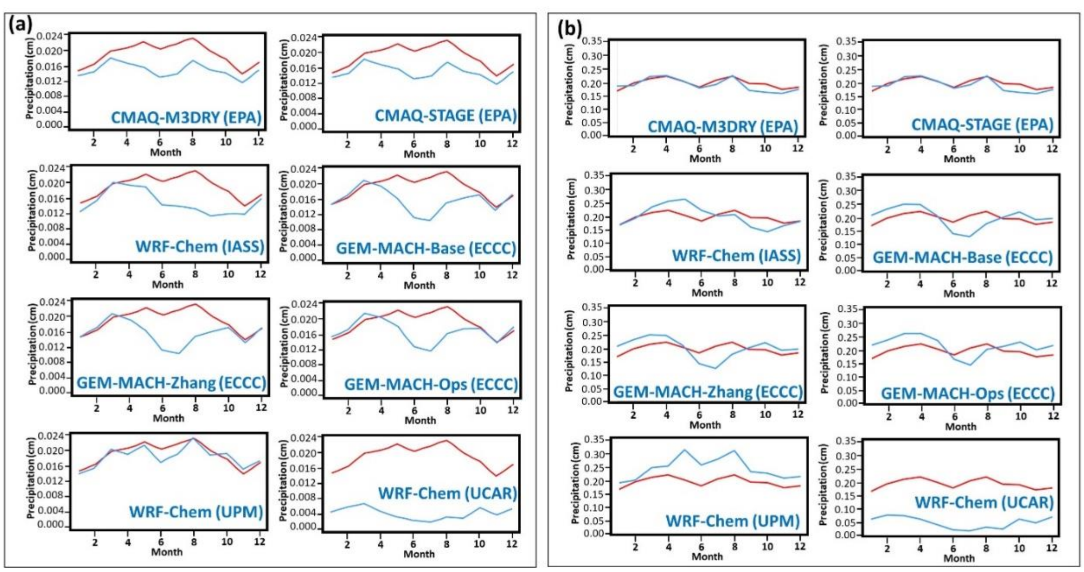

S8.0 Additional annual effective mass flux figures

Figure S19. Spatial distribution of annual effective mass flux of HNO_3 via cuticle resistance pathway, AQMEII4 NA models, 2016 (eq. ha^{-1} yr^{-1}).

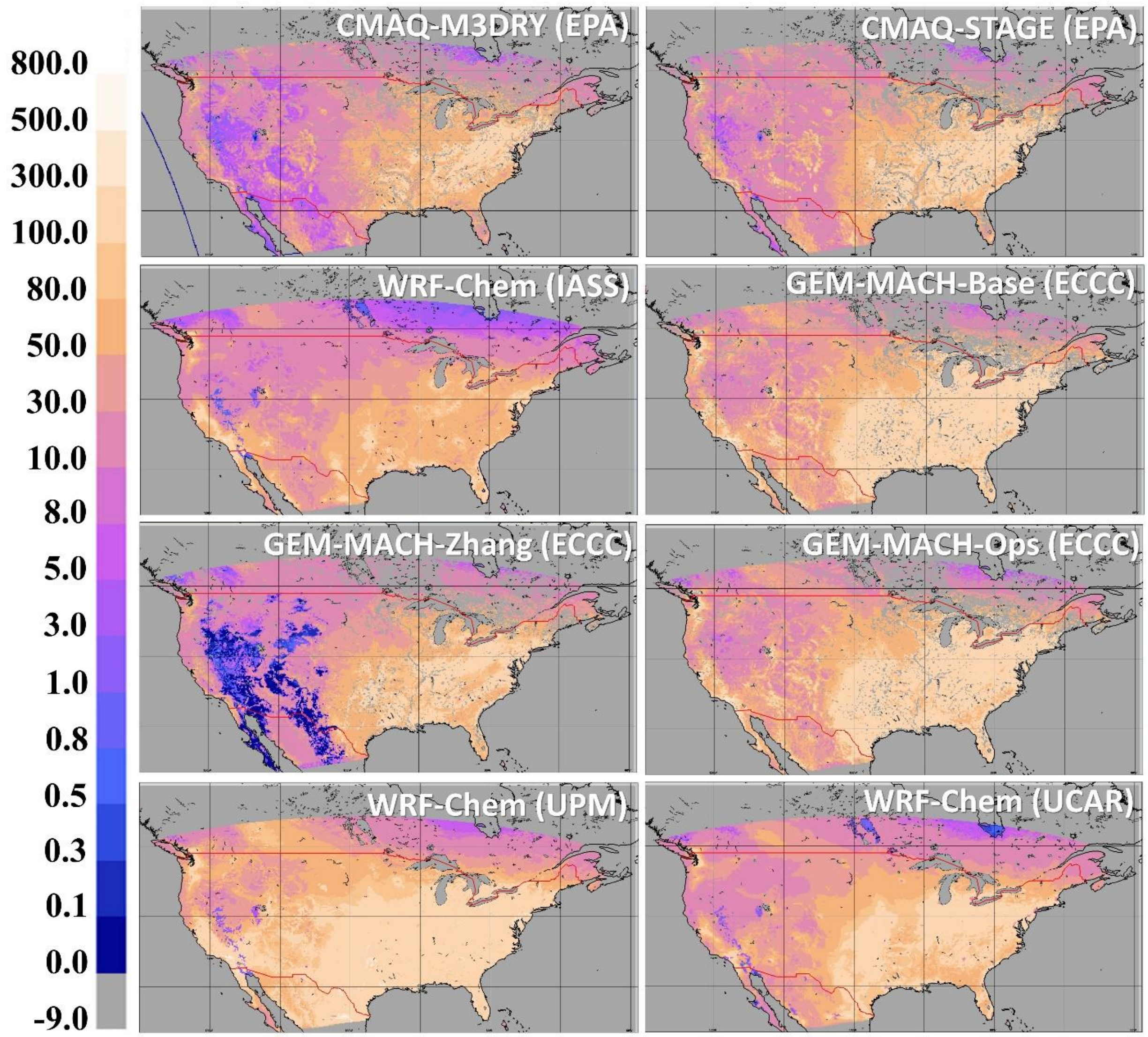

Figure S20. Spatial distribution of annual effective mass flux of HNO_3 via soil resistance pathway, AQMEII4 NA models, 2016 (eq. ha^{-1} yr^{-1}). Note that the CMAQ models incorporate lower canopy effective flux as part of the soil effective flux (see Figure SI14).

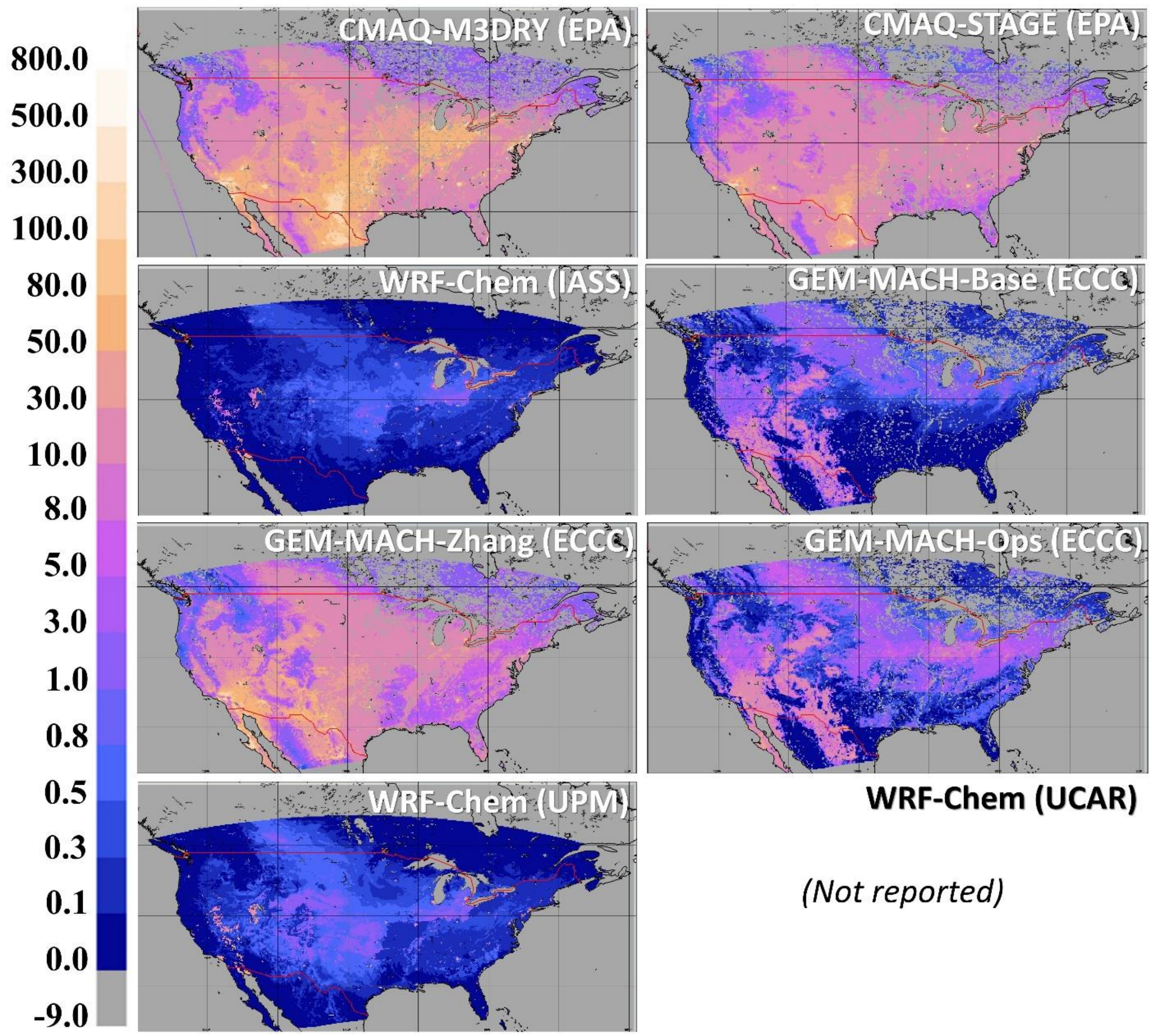

Figure S21. Spatial distribution of annual effective mass flux of HNO_3 via stomatal resistance pathway, AQMEII4 NA models, 2016 (eq. ha^{-1} yr^{-1}).

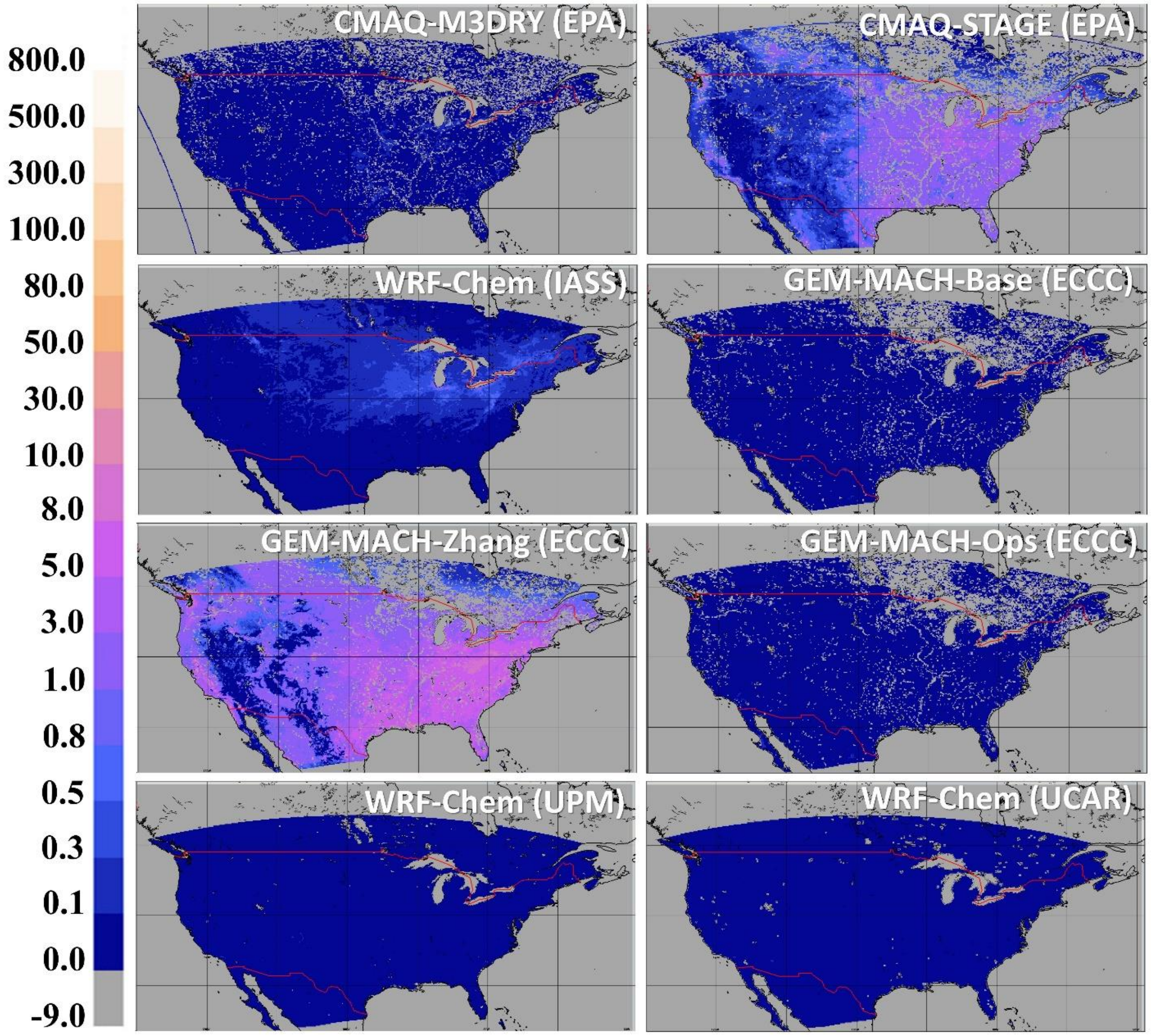

Figure S22. Spatial distribution of annual effective mass flux of HNO_3 via lower canopy resistance pathway, AQMEII4 NA models, 2016 (eq. ha^{-1} yr^{-1}).

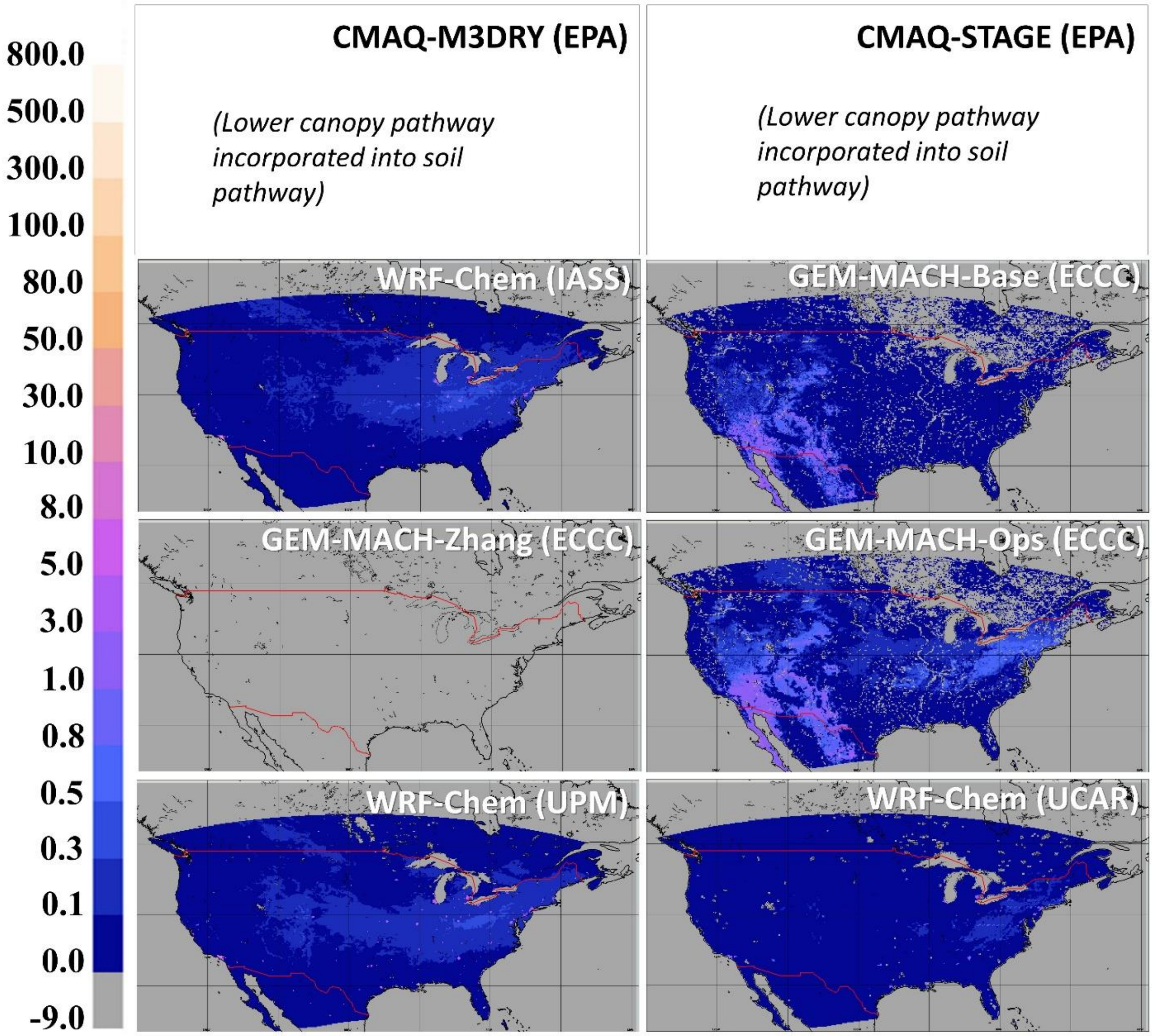

Figure S23. Spatial distribution of annual effective mass flux of SO_2 via cuticle (a) and (b) soil pathways, AQMEII4 EU models, 2010 (eq. ha^{-1} yr^{-1}).

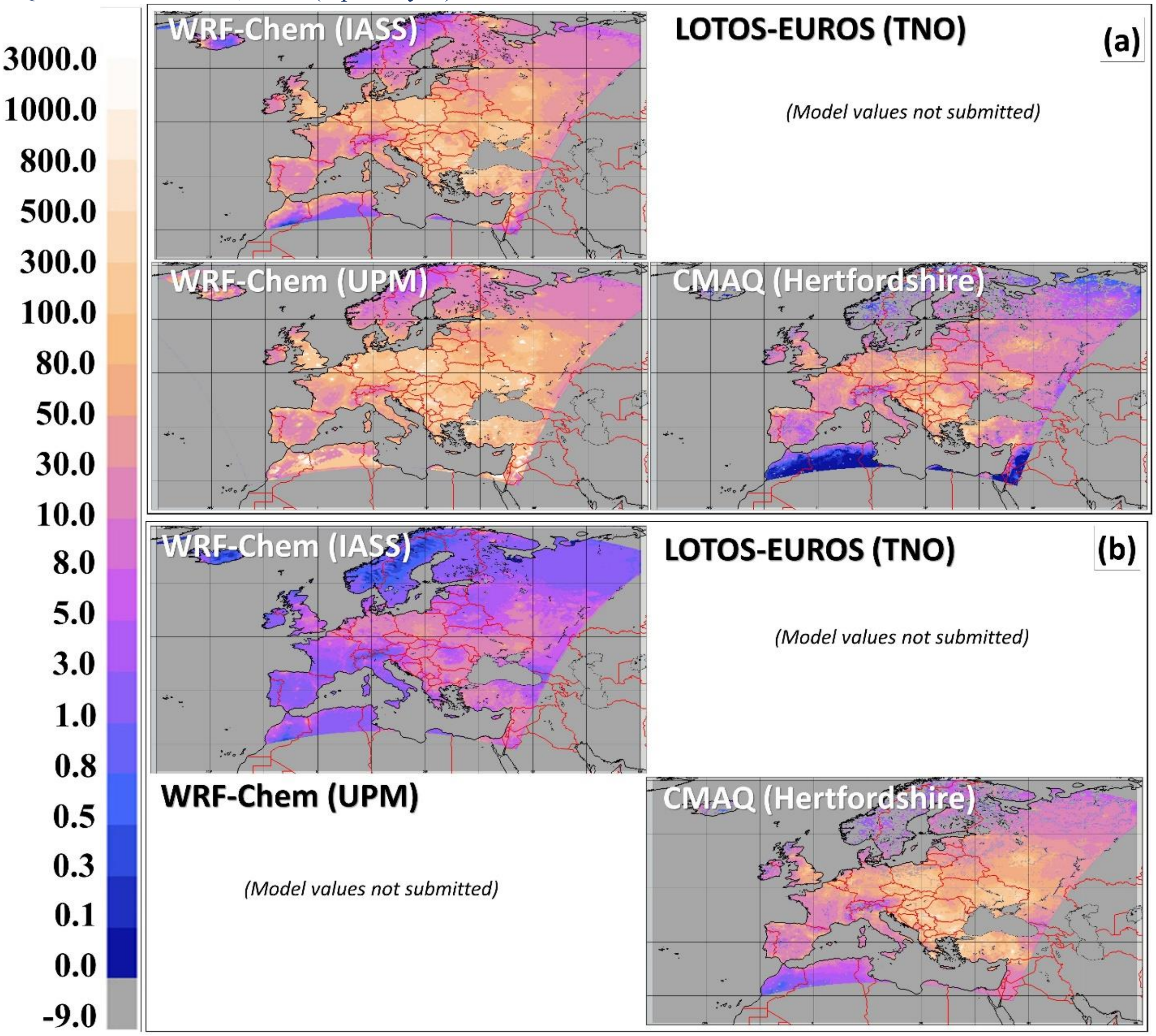

Figure S24. Spatial distribution of annual effective mass flux of SO_2 via stomatal (a) and (b) lower canopy pathways, AQMEII4 EU models, 2010 (eq. ha^{-1} yr^{-1}).

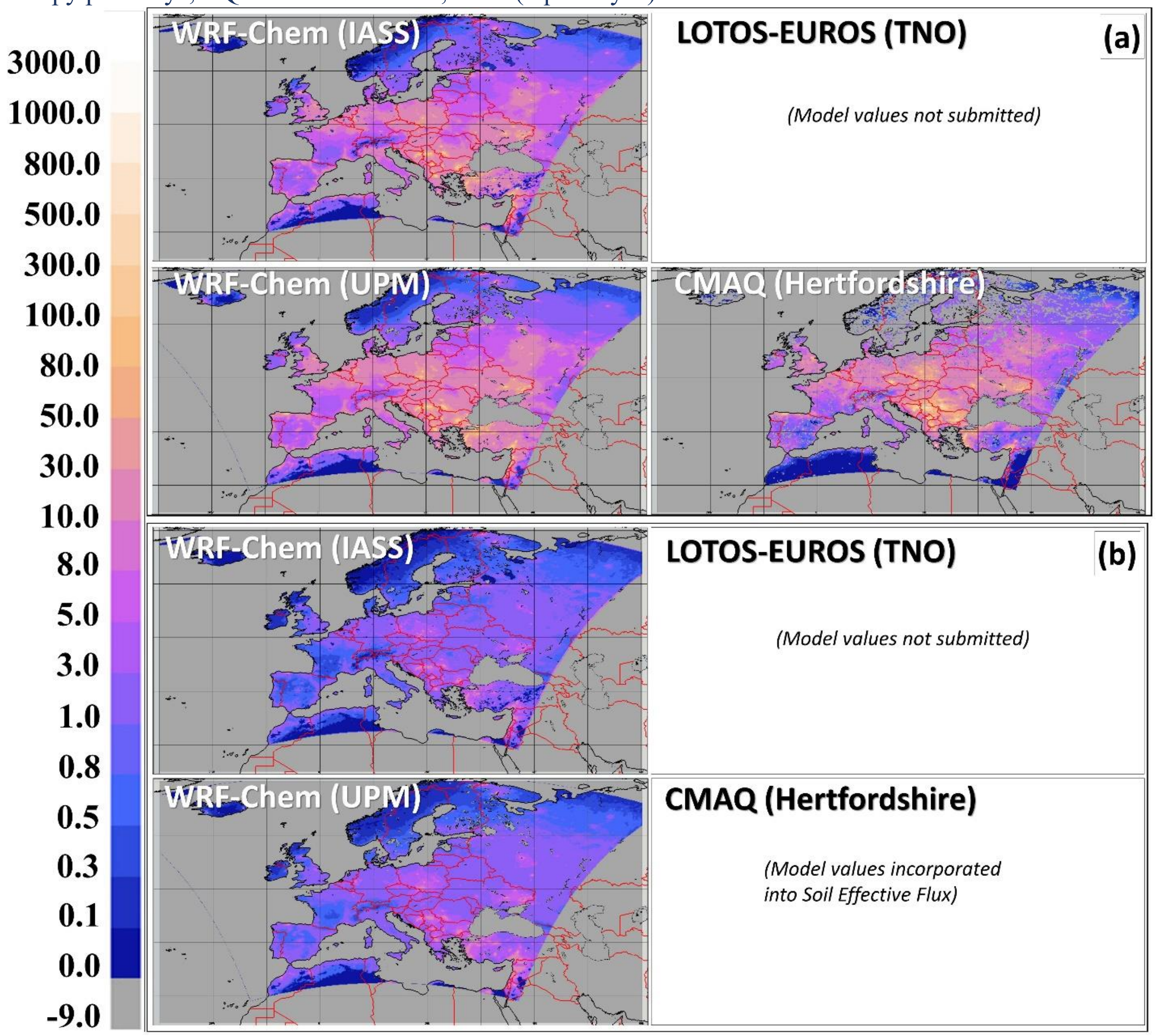

Figure S25. Spatial distribution of annual effective mass flux of HNO_3 via (a) cuticle, (b) soil pathways, AQMEII4 EU models, 2010 (eq. ha^{-1} yr^{-1}).

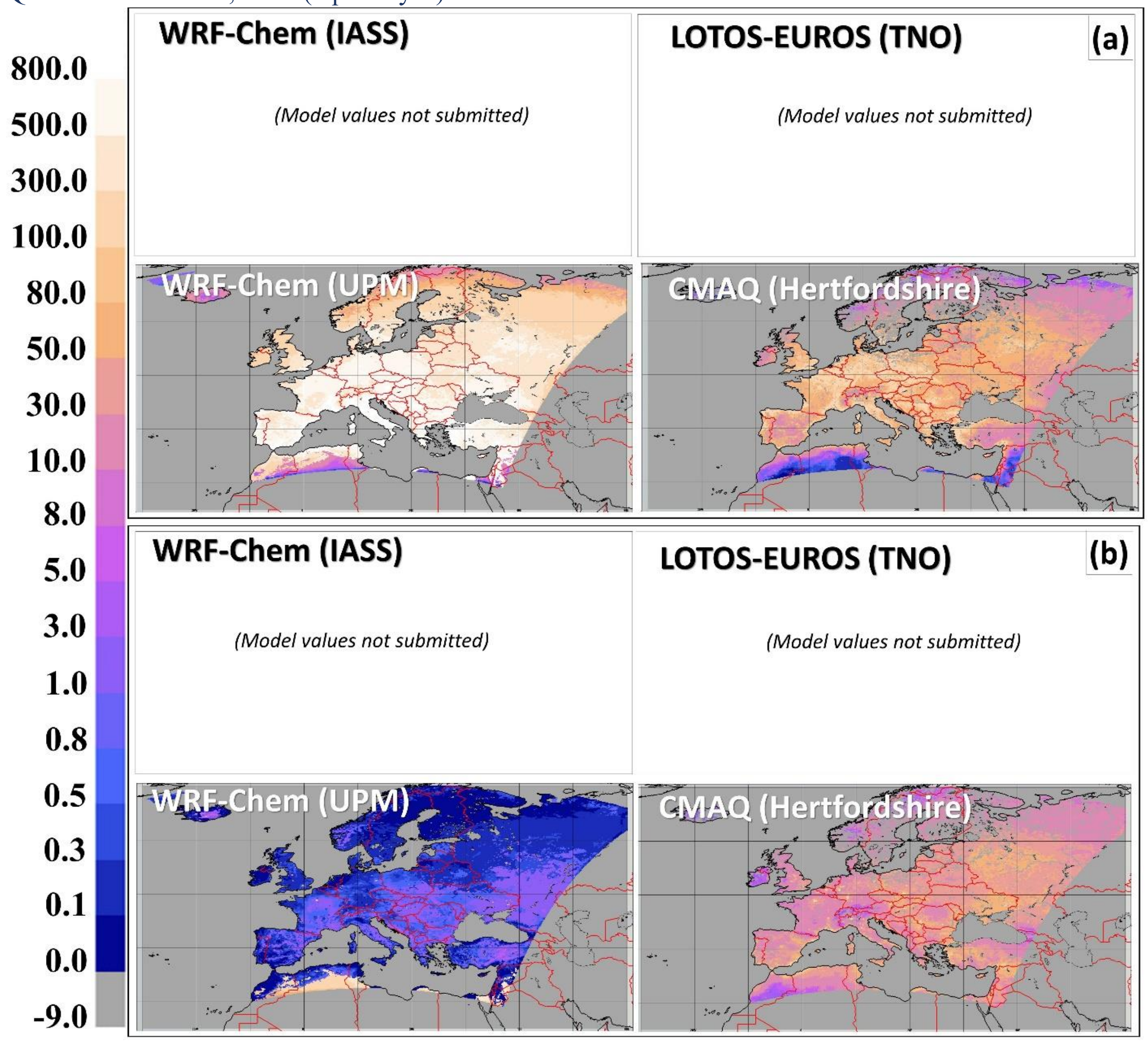

Figure S26. Spatial distribution of annual effective mass flux of HNO_3 via (a) stomatal resistance pathway, (b) lower canopy resistance pathway, AQMEII4 EU models, 2010 (eq. ha^{-1} yr^{-1}).